

# Towards More Suitable Personalization in Federated Learning via Decentralized Partial Model Training

Yifan Shi<sup>1,†</sup> Yingqi Liu<sup>2,†</sup> Yan Sun<sup>3</sup> Zihao Lin<sup>4</sup>

Li Shen<sup>5,\*</sup> Xueqian Wang<sup>1,\*</sup> Dacheng Tao<sup>3</sup>

<sup>1</sup>Tsinghua University; <sup>2</sup>Nanjing University of Science and Technology

<sup>3</sup>The University of Sydney; <sup>4</sup>Virginia Tech; <sup>5</sup>JD Explore Academy

shiyf21@mails.tsinghua.edu.cn; lyq@njut.edu.cn; ysun9899@uni.sydney.edu.au  
zihao@vt.edu; wang.xq@sz.tsinghua.edu.cn; {mathshenli,dacheng.tao}@gmail.com

## Abstract

Personalized federated learning (PFL) aims to produce the greatest personalized model for each client to face an insurmountable problem – data heterogeneity in real FL systems. However, almost all existing works have to face large communication burdens and the risk of disruption if the central server fails. Only limited efforts have been used in a decentralized way but still suffers from inferior representation ability due to sharing the full model with its neighbors. Therefore, in this paper, we propose a personalized FL framework with a decentralized partial model training called DFedAlt. It personalizes the “right” components in the modern deep models by alternately updating the shared and personal parameters to train partially personalized models in a peer-to-peer manner. To further promote the shared parameters aggregation process, we propose DFedSalt integrating the local Sharpness Aware Minimization (SAM) optimizer to update the shared parameters. It adds proper perturbation in the direction of the gradient to overcome the shared model inconsistency across clients. Theoretically, we provide convergence analysis of both algorithms in the general non-convex setting for decentralized partial model training in PFL. Our experiments on several real-world data with various data partition settings demonstrate that (i) decentralized training is more suitable for partial personalization, which results in state-of-the-art (SOTA) accuracy compared with the SOTA PFL baselines; (ii) the shared parameters with proper perturbation make partial personalized FL more suitable for decentralized training, where DFedSalt achieves most competitive performance.

## 1 Introduction

To solve a major challenge — the data heterogeneity problem, most works propose to achieve many personalized individual models for all clients rather than a single global model fitting the whole data distribution from all clients, called personalized federated learning (PFL) [27]. However, almost all existing works suffer from communication burdens and the risk of disruption if the central server fails in the centralized FL

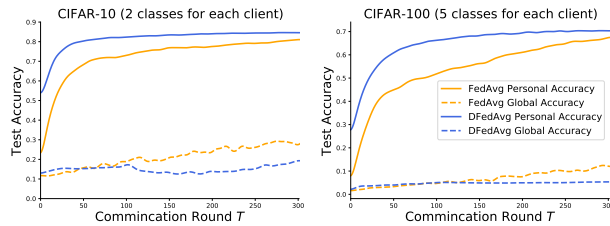


Figure 1: The training progress comparison between FedAvg and DFedAvg. DFedAvg can achieve competitive personal accuracy with fewer rounds than FedAvg compared with global accuracy.

\*Corresponding authors: Li Shen and Xueqian Wang. †Equal contribution.

(CFL) setting [4; 27]. Only limited efforts focusing on these issues have been used in a decentralized way for model aggregation, called the decentralized FL (DFL) setting. For instance, the works [26; 53; 10] leverage the full personalized model to communicate with the neighbors for each client in a peer-to-peer manner.

**Motivation.** Firstly, we comprehensively investigate the role of decentralized training in personalized FL (PFL) by conducting some toy experiments for FedAvg [44] and decentralized FedAvg (DFedAvg) [61] on both CIFAR-10 and CIFAR-100 datasets with a pathological partition approach in Figure 1, in which data distributions are very heterogeneous across clients — only 2 classes on CIFAR-10 and 5 classes on CIFAR-100 for each client, and a very sparse topology — Ring topology is applied on DFedAvg with 100 clients. It is clear that for one global model accuracy, the performance of DFL is worse than that of CFL. In contrast, personal accuracy in DFL is better than that in CFL. It indicates that the decentralized training method might be more suitable for PFL tasks. However, existing works focusing on a decentralized way in PFL [10; 53; 26], still face an inferior representation ability challenge in modern deep models due to losing unique information in each client, which is caused by full model aggregation with its neighbors [48]. Existing work in PFL [48] also provides a similar opinion — a fully personalized model may lead to “catastrophic forgetting” [43]. Therefore, a question arises:

*Can we seek out suitable personalization in FL via decentralized partial model training?*

**Contributions.** To seek out a better solution for PFL via sharing the partial “right” components selected with domain knowledge and unsharing the “unique” information in each client, we adopt the decentralized partial model training in PFL, named DFedAlt, which decomposes each local model as shared part and personalized part and then optimizes them alternatively in a decentralized manner. To the best of our knowledge, we are the first to explore decentralized partial personalization in PFL and face this inferior representation ability challenge by decomposing each local model and only averaging a shared part with its neighbors of each client. Furthermore, we propose an enhanced version of DFedAlt, called DFedSalt, which integrates local SAM optimizer [15] to update the shared parameters. Specifically, it searches for the shared parameters with uniformly low loss values by adding proper perturbation in the direction of the gradient, thereby promoting the process of local model aggregations in each client (see **Section 3**). Meanwhile, we present the non-trivially theoretical analysis for both DFedAlt and DFedSalt algorithms in the general non-convex setting (see **Section 4**), which can analyze the ill impact of the statistical heterogeneity and smoothness of loss functions on the convergence with partial personalization and SAM optimizer for the shared model. Empirically, we conduct extensive experiments on CIFAR-10, CIFAR-100, and Tiny-ImageNet datasets in non-IID settings with different data partitions, such as Dirichlet settings with various  $\alpha$  and pathological settings with various limited classes in each client. Experimental results confirm that our algorithms can achieve competitive performance relative to many SOTA PFL baselines (see **Section 5**).

In summary, we provide a comprehensive study focusing specifically on decentralized partial model personalization in PFL. Our main contributions lie in four-fold:

- We seek out suitable personalization in PFL with decentralized training and propose DFedAlt via alternately updating the shared part and personal part in a peer-to-peer manner.
- To further overcome the model inconsistency of the shared parameters, we propose DFedSalt, which enhances DFedAlt by integrating the local SAM optimizer into the shared parameters.
- We provide *convergence guarantees* for the DFedAlt and DFedSalt methods in the general non-convex setting with *decentralized partial participation* in PFL.
- We conduct *extensive experiments* on realistic data tasks with various data partition ways, evaluating the efficacy of our algorithms compared with some SOTA PFL baselines.

## 2 Related Work

**Personalized Federated Learning (PFL).** In recent years, the research works in PFL can be roughly divided into four categories: parameter decoupling [3; 9; 47], knowledge distillation [34; 40; 19], multi-task learning [24; 58], model interpolation [12; 13] and clustering [17; 54]. For instance, Ditto [38] adds a regularization term to address simultaneously robustness and fairness constraints in PFL

for federated multi-task learning. Recently, Fed-RoD [8] leverages a global body and two heads, e.g., the generic head trained with class-balanced loss and the personalized head trained with empirical loss, to generate both great generic performance and personalized performance. More details can be referred to in [63]. In this paper, we mainly focus on the parameter decoupling methods, which divide the model into a global shared part and a personalized part, also called *partial personalization*.

**Partial Personalization in FL.** Existing works demonstrate that partial personalization often outperforms full personalization. Specifically, FedPer [3] uses the one global body with many local heads approach and only shares the body layers with the server. After that, the entire model jointly is learned for each local client. FedRep [9] learns the entire model sequentially with the head updating first and the body later, and only shares the body layers with the server too. Where the linear convergence is also presented for a two-layer linear network. FedBABU [47] trains the global body with a fixed head for all clients and finally fine-tunes the personalized heads on the basis of the consensus body. And they [47] also explore empirically that mixing heads in heterogeneous scenarios will lead to the performance degradation of local models. FedSim and FedAlt are proposed in [48], they provide the first convergence analyses of both algorithms in the general nonconvex setting with partial participation, where FedAlt leverages the alternating update algorithm similar to FedRep, and FedSim uses the simultaneous update algorithm similar to FedPer.

**Decentralized Federated Learning (DFL).** Due to the participants having different hardware and network capabilities in the real federated system, DFL is an encouraging field of research that has repeatedly been reported as challenging in several review articles in recent years [4; 28; 35; 46; 64; 65; 70]. In DFL, the clients only connect with their neighbors and its goal is to make all local models tend to a unified model through peer-to-peer communication. For some applications, BrainTorrent [52] is the first serverless, peer-to-peer FL approach and applied to medical applications in a highly dynamic peer-to-peer FL environment. Similar to general FL methods such as [44], we discuss the DFL methods considering both multi-steps local iterations and various communication topologies.<sup>2</sup> Specifically, DFedAvg [61] applies the multiple local iterations with SGD and quantization method to reduce the communication cost and provide the convergence results in various convex settings. DisPFL [10] customizes the personalized model and pruned mask for each client to further lower the communication and computation cost. KD-PDFL [26] leverages knowledge distillation technique to empower each device so as to discern statistical distances between local models. The work in [53] presents lower bounds on the communication and local computation costs for this personalized FL formulation in a peer-to-peer manner. DFedSAM [56] integrates Sharpness Awareness Minimization (SAM) into DFL to improve the model consistency across clients.

The most related works to this paper lie in (i) CFL methods: FedPer [3], FedRep [9], FedBABU [47], Ditto [38], and Fed-RoD[8]; (ii) DFL methods: DFedAvgM [61], Dis-PFL [10], and DFedSAM [56]. However, in PFL, almost all existing works have to face large communication burdens and the risk of disruption if the central server fails. Only limited efforts have been used in a decentralized way but still suffers from poor representation ability due to sharing the full personalized model with its neighbors. Therefore, different from existing works, we try to seek out suitable personalization in FL via decentralized partial model training. Meanwhile, we provide the first convergence analysis on decentralized partial model personalization in FL, which is non-trivial.

### 3 Methodology

In this section, we define the problem setup for DFL and decentralized partial personalized models in PFL at first. After that, we present two algorithms: DFedAlt and DFedSalt in PFL, which leverages the decentralized partial model personalization technique to generate better representation ability while achieving SOTA performance relative to many related PFL methods.

#### 3.1 Problem Setup

**Decentralized Federated Learning (DFL).** We consider a typical setting of DFL with  $m$  clients, where each client  $i$  has the data distribution  $\mathcal{D}_i$ . Let  $w \in \mathbb{R}^d$  represent the parameters of a machine

<sup>2</sup>In decentralized/distributed training, they also focus on peer-to-peer communication, but one-step local iteration is adopted, due to the gradient computation being more focused than the communication burden. More detailed related works in decentralized/distributed training are placed in **Appendix A**.

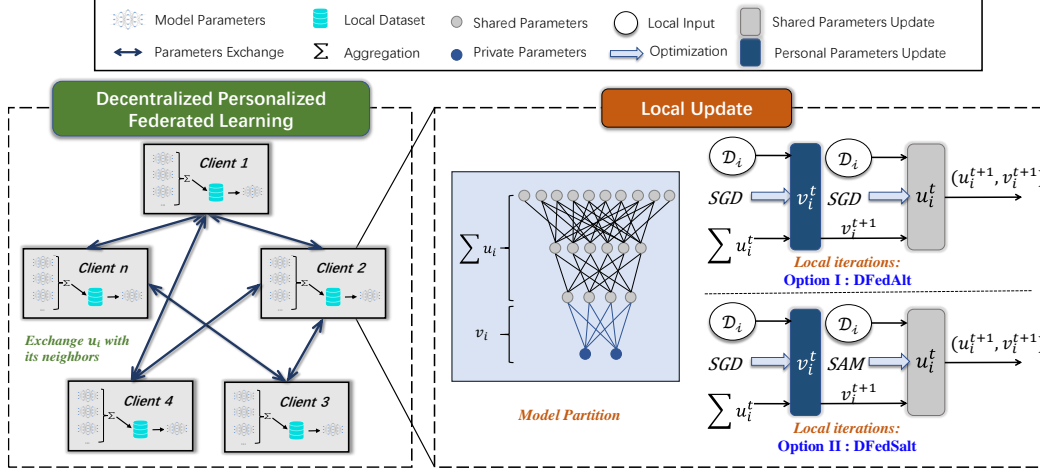


Figure 2: An overview of the proposed DFedAlt and DFedSalt frameworks.

learning model and  $F_i(w; \xi)$  is the local objective function associated with the training data samples  $\xi$ . Then the loss function associated with client  $i$  is  $F_i(w) = \mathbb{E}_{\xi \sim \mathcal{D}_i} F_i(w; \xi)$ . After that, a common objective of DFL is the following finite-sum stochastic non-convex minimization problem:

$$\min_{w \in \mathbb{R}^d} F(w) := \frac{1}{m} \sum_{i=1}^m F_i(w). \quad (1)$$

In the decentralized network topology, the communication between clients can be modeled as an undirected connected graph  $\mathcal{G} = (\mathcal{N}, \mathcal{V}, \mathbf{W})$ , where  $\mathcal{N} = \{1, 2, \dots, m\}$  represents the set of clients,  $\mathcal{V} \subseteq \mathcal{N} \times \mathcal{N}$  represents the set of communication channels, each connecting two distinct clients, and the gossip/mixing matrix  $\mathbf{W}$  records whether the communication connects or not between any two clients. As below, we present the definition of  $\mathbf{W}$ :

**Definition 1** (The gossip/mixing matrix [61]). *The gossip matrix  $\mathbf{W} = [w_{i,j}] \in [0, 1]^{m \times m}$  is assumed to have these properties: (i) (Graph) If  $i \neq j$  and  $(i, j) \notin \mathcal{V}$ , then  $w_{i,j} = 0$ , otherwise,  $w_{i,j} > 0$ ; (ii) (Symmetry)  $\mathbf{W} = \mathbf{W}^\top$ ; (iii) (Null space property)  $\text{null}\{\mathbf{I} - \mathbf{W}\} = \text{span}\{\mathbf{1}\}$ ; (iv) (Spectral property)  $\mathbf{I} \succeq \mathbf{W} \succ -\mathbf{I}$ . Under these properties, the eigenvalues of  $\mathbf{W}$  satisfies  $1 = |\lambda_1(\mathbf{W})| > |\lambda_2(\mathbf{W})| \geq \dots \geq |\lambda_m(\mathbf{W})|$ . And  $\lambda := \max\{|\lambda_2(\mathbf{W})|, |\lambda_m(\mathbf{W})|\}$  and  $1 - \lambda \in (0, 1]$  is the spectral gap of  $\mathbf{W}$ , which usually measures the degree of the network topology.*

**DFL with Partial Personalized Models.** Below, we present a general setting of DFL with *partial model personalization* for considering the communication overhead. Specifically, the model parameters are partitioned into two parts: the *shared* parameters  $u \in \mathbb{R}^{d_0}$  and the *personal* parameters  $v_i \in \mathbb{R}^{d_i}$  for  $i = 1, \dots, m$ . The full model on client  $i$  is denoted as  $w_i = (u_i, v_i)$ . To simplify presentation, we denote  $V = (v_1, \dots, v_m) \in \mathbb{R}^{d_1 + \dots + d_m}$ , and then our goal is to solve this problem:

$$\min_{u, V} F(u, V) := \frac{1}{m} \sum_{i=1}^m F_i(u, v_i), \quad (2)$$

where  $u$  denotes the consensus model averaged with all shared models  $u_i$ , that is  $u = \frac{1}{m} \sum_{i=1}^m u_i$ . Moreover, we consider the more general non-convex setting with local functions  $F_i(u_i, v_i) = \mathbb{E}_{\xi_i \sim \mathcal{D}_i} [F_i(u_i, v_i; \xi_i)]$ , and for brevity, also use  $\nabla_u$  and  $\nabla_v$  to represent stochastic gradients with respect to  $u_i$  and  $v_i$ , respectively.

In the DFL setting, the shared parameters  $u_i$  of each client  $i$  are sent out to the neighbors of client  $i$  from the neighborhood set with adjacency matrix  $\mathbf{W}$ , which records the communication connections between any two clients (communication topology). In contrast, the personal parameters  $v_i$  only perform multiple local iterations in each client  $i$  and do not be sent out.

### 3.2 DFedAlt and DFedSalt Algorithms

In this subsection, we present the DFedAlt and DFedSalt algorithms for solving problem (2). The detailed procedure and pipeline are presented in Algorithm 1 and Figure 2, respectively.

**DFedAlt.** To explore the possible partial personalization benefit of DFL, we present a useful partial personalization framework in DFL, named DFedAlt, which leverages the alternating update approach for model training. Specifically, the personal parameters  $v_i$  for each client perform multiple local iterations at first in line 6. After that, the shared parameters  $u_i$  perform multiple local iterations in line 10. After multiple local iterations of shared parameters  $u_i$  in each client  $i$ , the resulting parameters  $z_i^t \leftarrow u_i^{t,K_u}$  is sent to its neighbors in line 12. And then each client updates its shared parameters by averaging its neighbors' shared parameters (including itself).

#### An Enhanced Algorithm: DFedSalt.

In FL, the model inconsistency issue is a major challenge across clients due to data heterogeneity [56; 61], resulting in severe over-fitting of local models. In particular, sparse communication topology is also a key factor causing this issue in DFL [56]. Therefore, to further make partial personalization more suitable for DFL by decreasing the generalization error of shared parameters, we propose DFedSalt, which integrates the SAM optimizer into the local iteration update of shared parameters  $u_i$ . Specifically, we adopt proper perturbation in the direction of the local gradient of the shared parameters  $u_i$ . At first, the gradient  $\nabla_u F_i(u_i^{t,k}, v_i^{t+1}; \xi_i)$  of  $u_i$  is calculated on mini-batch data  $\xi_i$  for each client  $i$ . And then, we calculate the perturbation value in line 18, where  $\rho$  is a hyper-parameter for controlling the value of the perturbation radius. Finally, adding the perturbation term into the direction of gradient  $\nabla_u F_i(u_i^{t,k}, v_i^{t+1}; \xi_i)$  in line 18. The local averaging of  $u_i$  is the same as the DFedAlt algorithm.

## 4 Theoretical Analysis

In this section, we present the convergence analysis in DFedAlt and DFedSalt methods for the characterization of convergence speed and the exploration of how partial personalization and SAM optimizer work. Below, we state some general assumptions at first.

**Assumption 1** (Smoothness [48]). *For each client  $i = \{1, \dots, m\}$ , the function  $F_i$  is continuously differentiable. There exist constants  $L_u, L_v, L_{uv}, L_{vu}$  such that for each client  $i = \{1, \dots, m\}$ :*

- $\nabla_u F_i(u_i, v_i)$  is  $L_u$ -Lipschitz with respect to  $u_i$  and  $L_{uv}$ -Lipschitz with respect to  $v_i$
- $\nabla_v F_i(u_i, v_i)$  is  $L_v$ -Lipschitz with respect to  $v_i$  and  $L_{vu}$ -Lipschitz with respect to  $u_i$ .

We summarize the relative cross-sensitivity of  $\nabla_u F_i$  with respect to  $v_i$  and  $\nabla_v F_i$  with respect to  $u$  with the scalar

$$\chi := \max\{L_{uv}, L_{vu}\} / \sqrt{L_u L_v}.$$

**Assumption 2** (Bounded Variance [48]). *The stochastic gradients in Algorithm 1 have bounded variance. That is, for all  $u_i$  and  $v_i$ , there exist constants  $\sigma_u$  and  $\sigma_v$  such that*

$$\mathbb{E}[\|\nabla_u F_i(u_i, v_i; \xi_i) - \nabla_u F_i(u_i, v_i)\|^2] \leq \sigma_u^2, \quad \mathbb{E}[\|\nabla_v F_i(u_i, v_i; \xi_i) - \nabla_v F_i(u_i, v_i)\|^2] \leq \sigma_v^2.$$

**Assumption 3** (Partial Gradient Diversity [48]). *There exist a constant  $\delta \geq 0$  such that*

$$\frac{1}{m} \sum_{i=1}^m \|\nabla_u F_i(u_i, v_i) - \nabla_u F(u_i, V)\|^2 \leq \delta^2, \quad \forall u_i, V.$$

---

#### Algorithm 1: DFedAlt and DFedSalt

---

**Input** : Total number of devices  $m$ , total number of communication rounds  $T$ , local learning rate  $\eta_u$  and  $\eta_v$ , total number of local iterates  $K_u$  and  $K_v$ .

**Output** : Personalized model  $u_i^T$  and  $v_i^T$  after the final communication of all clients.

```

1 Initialization: Randomly initialize each device's shared
  parameters  $u_i^0$  and personal parameters  $v_i^0$ .
2 for  $t = 0$  to  $T - 1$  do
3   for client  $i$  in parallel do
4     Set  $u_i^{t,0} \leftarrow u_i^t$  and sample a batch of local data  $\xi_i$ 
      and calculate local gradient iteration.
5     for  $k = 0$  to  $K_v - 1$  do
6       Perform personal parameters  $v_i$  update:
7        $v_i^{t,k+1} = v_i^{t,k} - \eta_v \nabla_v F_i(u_i^{t,0}, v_i^{t,k}; \xi_i)$ .
8     end
9      $v_i^{t+1} \leftarrow v_i^{t,K_v}$ .
10    for  $k = 0$  to  $K_u - 1$  do
11      Update shared parameters  $u_i$  via Option I or II.
12    end
13     $z_i^t \leftarrow u_i^{t,K_u}$ . Receive neighbors' shared models  $z_j^t$ 
      with adjacency matrix  $\mathbf{W}$ :
14     $u_i^{t+1} = \sum_{l \in \mathcal{N}(i)} w_{i,l} z_l^t$ .
15  end
16 Option I: (DFedAlt) Find a minimum for  $u_i$  with SGD
17  $u_i^{t,k+1} = u_i^{t,k} - \eta_u \nabla_u F_i(u_i^{t,k}, v_i^{t+1}; \xi_i)$ .
18 Option II: (DFedSalt). Find a flat minimum for  $u_i$  with SAM
19  $\epsilon(u_i^{t,k}) = \rho \frac{\nabla_u F_i(u_i^{t,k}, v_i^{t+1}; \xi_i)}{\|\nabla_u F_i(u_i^{t,k}, v_i^{t+1}; \xi_i)\|_2}$ .
20  $u_i^{t,k+1} = u_i^{t,k} - \eta_u \nabla_u F_i(u_i^{t,k} + \epsilon(u_i^{t,k}), v_i^{t+1}; \xi_i)$ .

```

---

The above assumptions are mild and commonly used in the convergence analysis of FL [61; 56; 16; 67; 6; 50; 23; 49].

**About the Challenges of Convergence Analysis.** Due to the central server being discarded, various communication connections will become an important factor for decentralized optimization. Furthermore, communication is more careful in general classical FL scenarios rather than computation [44; 37; 27; 49]. So the client adopts multi-step local iterations such as FedAvg [44], which may lead to the local gradient failing to be unbiased. Because of these factors, technical difficulty exists in our theoretical analysis. How to analyze the convergence of decomposed model parameters while delivering the impact of communication topology. In this paper, we adopt the averaged shared parameter  $\bar{u}^t = \frac{1}{m} \sum_{i=1}^m u_i^t$  of all clients to be the approximated solution of problem (2) due to only the shared parameters being communicated with the neighbors [61; 56]. Now, we present the rigorous convergence rate of DFedAlt and DFedSalt algorithms as follows.

**Theorem 1** (Convergence Analysis for DFedAlt). *Under assumptions 1-3 and definition 1, the local learning rates satisfy  $\eta_u = \mathcal{O}(1/L_u K_u \sqrt{T})$ ,  $\eta_v = \mathcal{O}(1/L_v K_v \sqrt{T})$ ,  $F^*$  is denoted as the minimal value of  $F$ , i.e.,  $F(\bar{u}, V) \geq F^*$  for all  $\bar{u} \in \mathbb{R}^d$ , and  $V = (v_1, \dots, v_m) \in \mathbb{R}^{d_1 + \dots + d_m}$ . Let  $\bar{u}^t = \frac{1}{m} \sum_{i=1}^m u_i^t$  and denote  $\Delta_u^t$  and  $\Delta_v^t$  as:*

$$\Delta_u^t = \|\nabla_u F(\bar{u}^t, V^{t+1})\|^2, \quad \text{and} \quad \Delta_v^t = \frac{1}{m} \sum_{i=1}^m \|\nabla_v F_i(u_i^t, v_i^t)\|^2.$$

Therefore, we have the convergence rate as below:

$$\frac{1}{T} \sum_{i=1}^T \left( \frac{1}{L_u} \mathbb{E}[\Delta_u^t] + \frac{1}{L_v} \mathbb{E}[\Delta_v^t] \right) \leq \mathcal{O} \left( \frac{F(\bar{u}^1, V^1) - F^*}{\sqrt{T}} + \frac{\sigma_1^2}{\sqrt{T}} + \frac{\sigma_2^2}{T(1-\lambda)^2} \right), \quad (3)$$

where

$$\sigma_1^2 = \frac{\sigma_v^2(L_v + 1)}{L_v^2} + \frac{L_{vu}^2(\sigma_u^2 + \delta^2)}{L_u^2} = \frac{\sigma_v^2(L_v + 1)}{L_v^2} + \frac{\chi^2 L_v(\sigma_u^2 + \delta^2)}{L_u}, \quad \sigma_2^2 = \frac{\sigma_u^2 + \delta^2}{L_u}.$$

**Remark 1.** These variables have a significant influence on the convergence bound. Specifically, measuring the statistical heterogeneity, such as local variance  $\sigma_u^2, \sigma_v^2$  and global diversity, the smoothness of local loss functions such as  $L_u, L_v$ , and  $L_{vu}$ , and the communication topology measured by  $1 - \lambda$ .

**Theorem 2** (Convergence Analysis for DFedSalt). *Under assumptions 1-3 and definition 1, the local learning rates satisfy  $\eta_u = \mathcal{O}(1/L_u K_u \sqrt{T})$ ,  $\eta_v = \mathcal{O}(1/L_v K_v \sqrt{T})$ . Let  $\bar{u}^t = \frac{1}{m} \sum_{i=1}^m u_i^t$  and denote  $\Delta_u^t$  and  $\Delta_v^t$  as Theorem 1. When the perturbation amplitude  $\rho$  is proportional to the learning rate, e.g.,  $\rho = \mathcal{O}(1/\sqrt{T})$ , the sequence of outputs  $\Delta_u^t$  and  $\Delta_v^t$  generated by DFedSalt, we have:*

$$\frac{1}{T} \sum_{i=1}^T \left( \frac{1}{L_u} \mathbb{E}[\Delta_u^t] + \frac{1}{L_v} \mathbb{E}[\Delta_v^t] \right) \leq \mathcal{O} \left( \frac{F(\bar{u}^1, V^1) - F^*}{\sqrt{T}} + \frac{\sigma_v^2(L_v + 1)}{L_v^2 \sqrt{T}} + \frac{L_u}{T} + \frac{\sigma^2 L_{vu}^2}{T^{1/2}(1-\lambda)^2} + \frac{\sigma^2 L_u}{T(1-\lambda)^2} \right), \quad (4)$$

where  $\mathcal{O}(\sigma^2) = \mathcal{O}\left(\frac{\rho^2}{K_u} + \frac{\sigma_u^2 + \delta^2}{L_u^2}\right) = \mathcal{O}\left(\frac{1}{K_u T} + \frac{\sigma_u^2 + \delta^2}{L_u^2}\right)$  when  $\rho = \mathcal{O}(\frac{1}{\sqrt{T}})$ .

**Remark 2.** It is clear that the bound is facilitated via SAM optimizer from the smoothness-enabled perspective, such as  $L_u^2$  and  $L_{vu}^2$ . Thus, the shared model  $u_i$  may be flatter, thereby decreasing the generalization error of the whole model  $w_i = (u_i, v_i)$ . Finally, the shared parameters  $u_i$  aggregation process is promoted, thereby achieving better performance.

## 5 Experiments

In this section, we conduct extensive experiments to verify the effectiveness of the proposed DFedAlt and DFedSalt algorithms. Below, we first introduce the experimental setup.

### 5.1 Experiment Setup

**Dataset and Data Partition.** We evaluate the performance of our approaches on CIFAR-10, CIFAR-100 [30], and Tiny-ImageNet [32] datasets in the Dirichlet distribution setting and Pathological setting, where CIFAR-10 and CIFAR-100 are two real-life image classification datasets with total 10 and 100 classes. And all detailed experiments on the Tiny-ImageNet dataset are placed in **Appendix**

Table 1: Test accuracy (%) on CIFAR-10 &amp; 100 in both Dirichlet and Pathological distribution settings.

Algorithm	CIFAR-10				CIFAR-100			
	Dirichlet		Pathological		Dirichlet		Pathological	
	$\alpha = 0.1$	$\alpha = 0.3$	$c = 2$	$c = 5$	$\alpha = 0.1$	$\alpha = 0.3$	$c = 5$	$c = 10$
Local	78.96 $\pm$ .42	63.20 $\pm$ .28	85.16 $\pm$ .18	68.56 $\pm$ .35	39.38 $\pm$ .33	22.59 $\pm$ .49	71.34 $\pm$ .46	53.15 $\pm$ .31
FedAvg	84.17 $\pm$ .28	80.02 $\pm$ .20	84.99 $\pm$ .11	81.18 $\pm$ .27	57.35 $\pm$ .03	55.12 $\pm$ .06	69.29 $\pm$ .43	66.10 $\pm$ .48
FedPer	88.57 $\pm$ .09	84.06 $\pm$ .29	90.94 $\pm$ .24	86.97 $\pm$ .35	54.23 $\pm$ .14	34.07 $\pm$ .76	78.48 $\pm$ .93	70.38 $\pm$ .02
FedRep	88.78 $\pm$ .40	84.50 $\pm$ .05	91.09 $\pm$ .12	86.22 $\pm$ .51	44.02 $\pm$ .98	26.88 $\pm$ .49	78.77 $\pm$ .19	68.15 $\pm$ .43
FedBABU	87.79 $\pm$ .53	83.26 $\pm$ .09	91.32 $\pm$ .15	84.90 $\pm$ .24	60.23 $\pm$ .07	52.37 $\pm$ .82	77.50 $\pm$ .33	69.81 $\pm$ .12
Fed-RoD	89.15 $\pm$ .12	85.68 $\pm$ .08	90.10 $\pm$ .04	87.81 $\pm$ .45	65.79 $\pm$ .05	58.54 $\pm$ .69	80.50 $\pm$ .45	73.59 $\pm$ .15
Ditto	80.22 $\pm$ .10	73.51 $\pm$ .04	84.96 $\pm$ .40	75.59 $\pm$ .32	48.85 $\pm$ .54	48.65 $\pm$ .50	69.48 $\pm$ .45	60.77 $\pm$ .30
DFedAvgM	87.39 $\pm$ .13	82.60 $\pm$ .18	90.72 $\pm$ .08	84.69 $\pm$ .25	59.76 $\pm$ .69	54.98 $\pm$ .48	76.70 $\pm$ .59	71.08 $\pm$ .52
Dis-PFL	87.77 $\pm$ .46	82.71 $\pm$ .28	88.19 $\pm$ .47	82.29 $\pm$ .61	56.06 $\pm$ .20	46.65 $\pm$ .18	71.79 $\pm$ .42	65.35 $\pm$ .10
DFedSAM	84.96 $\pm$ .30	77.36 $\pm$ .11	90.14 $\pm$ .22	83.05 $\pm$ .40	58.21 $\pm$ .53	47.80 $\pm$ .49	74.25 $\pm$ .17	67.34 $\pm$ .43
DFedAlt	88.85 $\pm$ .21	86.50 $\pm$ .05	91.26 $\pm$ .23	86.85 $\pm$ .37	66.26 $\pm$ .25	57.66 $\pm$ .42	78.78 $\pm$ .41	72.19 $\pm$ .21
DFedSalt	<b>91.08</b> $\pm$ .34	<b>87.67</b> $\pm$ .22	<b>92.20</b> $\pm$ .14	<b>88.34</b> $\pm$ .31	<b>67.03</b> $\pm$ .36	<b>58.73</b> $\pm$ .19	<b>80.82</b> $\pm$ .33	<b>74.50</b> $\pm$ .35

B.3 due to the limited space. We partition the training and testing data according to the same Dirichlet distribution  $\text{Dir}(\alpha)$  such as  $\alpha = 0.1$  and  $\alpha = 0.3$  for each client followed by [22]. Specifically, the smaller the  $\alpha$  is, the more heterogeneous the setting is. Meanwhile, for each client, we sample 2 and 5 classes from a total of 10 classes on CIFAR-10, and 5 and 10 classes from a total of 100 classes on CIFAR-100, respectively [71]. Where the number of sampling classes is represented as “c” in Table 1 and the fewer classes each client owns, the more heterogeneous the setting is.

**Baselines and Backbone.** We compare the proposed methods with many baselines in both CFL and DFL. For instance, Local is the simplest method where each client only conducts training on their own data without communicating with other clients. And CFL methods include FedAvg [44], FedPer [3] (aka. FedSim [48]), FedRep [9] (aka. FedAlt [48]), FedBABU [47], Fed-RoD [8] and Ditto [38]. For DFL methods, we take DFedAvgM [61], Dis-PFL [11], DFedSAM [56] as our baselines. All methods are evaluated on ResNet-18 [20] and replace the batch normalization with the group normalization followed by [66; 11; 56] to avoid unstable performance. For the partial PFL methods, we set the lower linear layers (close to output) as the personal part responsible for complex pattern recognition, and the rest upper layer (close to input) as the shared part focusing on feature extraction. Note that we compare the personal test accuracy for all methods since our goal is to solve PFL.

**Implementation Details.** We keep the same experiment setting for all baselines and perform 500 communication rounds. The number of client sizes is 100. The client sampling ratio is 0.1 in CFL, while each client communicates with 10 neighbors in PFL accordingly. The batchsize is 128 and the number of local epochs is 5. For DFedAlt and DFedSalt, the local epochs for the shared parameters are 5, while the local epochs of the personal parameters are 1 on Dirichlet dataset and 5 on Pathological dataset. We set SGD [51; 59] as the base local optimizer with a learning rate  $\eta_v = 0.001$  for the personal and  $\eta_u = 0.1$  for shared parameters update with a decay rate of 0.005 and local momentum of 0.9. Additionally, the weight perturbation ratio in DFedSalt is set to  $\rho = 0.7$ . We run each experiment 3 times with different random seeds and report the mean accuracy with variance for each method. More details of the baselines can be found in **Appendix B**.

## 5.2 Performance Evaluation

**Comparison with the baselines.** As shown in Table 1 and Figure 3, the proposed DFedAlt and DFedSalt outperform other baselines with the best stability and perform well in severe data heterogeneity scenarios. It significantly proves that decentralized training is more suitable for PFL than centralized training. Specifically, on the CIFAR-10 dataset, DFedAlt and DFedSalt achieve 87.67% and 86.50% on the Dirichlet-0.3 setups, 0.82% and 1.99% ahead of the best comparing CFL method Fed-RoD. On the CIFAR-100 dataset, DFedSalt achieves at least 0.32% and 0.91% improvement from the other baselines on the Pathological-5 and Pathological-10 settings. The effect of the hyper network in Fed-RoD is remarkable but partial model personalization in the decentralized scenario can obtain greater gains than it. DFedAlt and DFedSalt focus on local optimization and absorb the feature extraction capabilities learned by other users on their own data. So they maintain the classified head more adapted to the local data for each client with a stronger feature extractor.



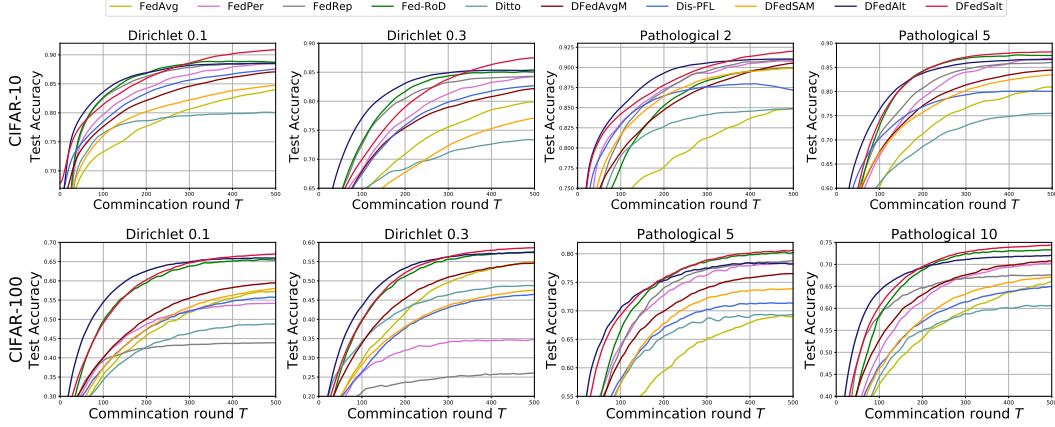


Figure 3: Test accuracy on CIFAR-10 (first line) and CIFAR-100 (second line) with heterogenous data partitions.

**Discussion on the heterogeneous setting.** We discuss two different data heterogeneity of Dirichlet distribution and Pathological distribution in Table 1, and we further prove the effectiveness and robustness of the proposed methods. In Dirichlet distribution, since the local training is hard to cater for all classes inside clients, the accuracy decreases with the level of heterogeneity decreasing. On CIFAR-10, when the heterogeneity increases from 0.1 to 0.3, Fed-RoD drops from 89.15% to 85.68%, while DFedSalt drops about 3.41% to 87.67%, meaning its strong adaptability and stability for several heterogeneous settings. Pathological distribution defines limited classes for each client which is a higher level of heterogeneity. In detail, DFedSalt is 0.88% ahead of the best compared CFL method on CIFAR-10 with only 2 categories per client and 0.91% ahead on CIFAR-100 dataset with only 10 categories per client. The comparisons confirm that the proposed methods could achieve better performance in the strong heterogeneity.

**Convergence speed.** We illustrate the convergence speed for all baselines via the learning curves under different settings in Figure 3 and collect the communication rounds for each method to reach a target accuracy (acc@) in Table 2. The results show that DFedAlt achieves the fastest convergence speed among the comparison methods, which benefits from the decentralized training mode and alternate update a lot. In comparison with the indirect interaction methods in CFL, which pass information through a central node, the direct information interaction in DFL can speed up the convergence rate for personalized problems. Also, the difference between DFedAlt and DFedAvgM indicates that the convergence speed of alternate updating is faster than uniform updating. Besides, Figure 4 also reveals that the fully-connected case may outperform other communication topologies in convergence speed. This can be attributed to the increased communication information per round, which has also been verified in [29; 11]. Notably, we target the setting where the busiest node’s communication bandwidth is restricted for fairness when compared with the CFL methods.

Table 2: The required communication rounds when achieving the target accuracy (%).

Algorithm	CIFAR-10		CIFAR-100	
	Dir-0.3	Pat-2	Dir-0.3	Pat-10
	acc@80	acc@90	acc@45	acc@65
FedAvg	-	-	234	456
FedPer	262	343	-	246
FedRep	189	322	-	225
FedBABU	270	312	261	314
Fed-RoD	170	462	133	148
Ditto	-	-	279	-
DFedAvgM	354	439	192	230
Dis-PFL	307	-	368	492
DFedSAM	-	465	367	344
DFedAlt	<b>131</b>	<b>224</b>	<b>111</b>	<b>113</b>
DFedSalt	160	280	131	139

**Discussion on communication topologies.** In practice, the clients are often connected with pre-given topologies and have different computing and communication capabilities, named heterogeneous clients. For decentralized methods, comparing the performance of various communication topologies will help us evaluate the performance of the methods with heterogeneous clients. Figure 4 shows the performances of each decentralized method in various communication

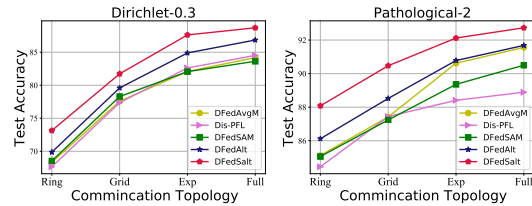


Figure 4: Personal test accuracy (%) in various network topologies for the DFL methods on CIFAR-10.



topologies on the CIFAR-10 dataset. The sparse degree of the communication topology from sparse to compact are Ring, Grid, Exp (aka. exponential), and Full (aka. full-connected), and the performance of all the methods improves correspondingly with the communication topology compacter. Besides, we find that the proposed DFedAlt and DFedSalt perform extremely well in various communication topologies. Specifically, in the Dirichlet setting, DFedAlt and DFedSalt outperform other baselines from 1.31%-5.00%. In the pathological setting, the accuracy gap between the Ring and Full topology of DFedAvg, DFedAlt, and DFedSalt is 6.44%, 5.56%, and 4.65%, respectively. This indicates that the DFedAlt and DFedSalt are more robust and suitable for the DFL setting.

### 5.3 Ablation Study

#### Integrating SAM into the shared model $u_i$ or personal model $v_i$ or whole model $(u_i, v_i)$ .

We investigate the effect of adding the SAM optimizer to different parts with different data heterogeneity on the CIFAR-10 dataset. From Table 3, DfedSalt-U (SAM only for the shared model, dubbed as “body”) achieves the best in Dirichlet setting and DFedSalt-UV (adding SAM to both shared and personal parts) achieves the best in Pathological setting. From the difference between DFedAlt, DFedSalt-U and DFedSalt-UV, we observe that the SAM optimizer can uniformly reduce the inconsistency of the feature extractor among clients and improve the feature extraction ability of the shared parts. Besides, the comparison from DFedAlt, DFedSalt-V (SAM only for the personal model, dubbed as “head”) and DFedSalt-UV illustrates that the benefits of adding SAM to the personal model may be sensitive to the data distribution and hyperparameter setup. Thus, in the main experiments, we set DFedSalt-U as our default algorithm and denote it as DFedSalt.

Table 3: Test accuracy (%) of different model parts with the SAM optimizer.

Algorithm	Body	Head	Dirichlet	Pathological
DFedAlt			86.50	91.26
DFedSalt-U	✓		<b>87.67</b>	92.20
DFedSalt-V		✓	86.46	91.50
DFedSalt-UV	✓	✓	87.43	<b>92.58</b>

**Effectiveness of local epochs.** In Figure 5, we illustrate the effect of local epochs for the personal parameters in different heterogeneity scenarios on the CIFAR-10 dataset after 200 communication rounds. For the Dirichlet scenarios, with fixed local epochs of 5 for the shared parameters, more local epochs (i.e., larger  $K_v$ ) for the personal parameters will damage the performance. That means fewer local epochs for the personal improve the shared part more and the personal part with less relative variance per user also fits well on local data. While in the Pathological scenarios, a more heterogeneous distribution for each client, the local epochs for the personal parameters must be a trade-off to improve the extraction ability of the shared part and adapt the personal part to the local data.

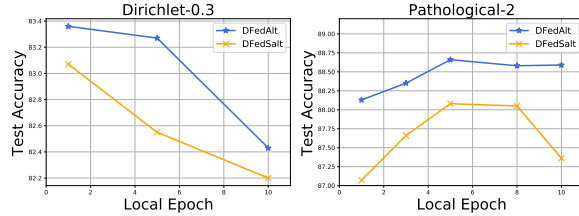


Figure 5: Effect of the local epochs for the personal parameters  $v_i$  in client  $i$ .

**Number of participated clients.** We compare the performance between different numbers of client participation of {20, 50, 100, 200} on CIFAR-10 with Dirichlet  $\alpha = 0.3$  in Figure 6. It is clearly seen that the test performance will get a great margin with the participation of clients decreasing, which means that the more training data each client owns, the better performance it will achieve.

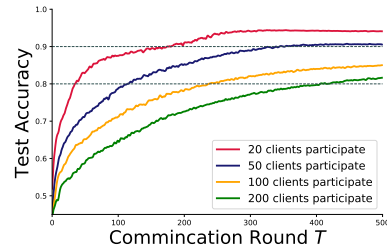


Figure 6: Effect of the participated clients size.

## 6 Conclusion

In this paper, we propose two novel methods — DFedAlt and DFedSalt for PFL, which improve the representation ability via adopting decentralized partial model personalization to seek out suitable personalization in FL. It efficiently personalizes the “right” components in the deep modern models and alternatively updates the shared parameters and personal parameters in a peer-to-peer manner. For theoretical findings, we present the convergence rate in the stochastic non-convex setting for DFedAlt and DFedSalt. Empirical results also verify the superiority of our approaches.

**Limitations.** In the current version, we mainly focus on the optimizer problem in personalized federated learning and have not explored further research and analysis on the generalization ability of the proposed methods. We will perform continuous research in this aspect in future work.

**Broader Impacts.** In this paper, we analyze and explore the main problems existing in personalized federated learning: single point of failure, communication burden, and poor representation ability. And we adopt the decentralized partial model personalization technique to alleviate the above-mentioned problems, dubbed as DFedAlt and DFedSalt. Meanwhile, we give theoretical convergence analysis and extensive experiments, these attempts indicate the effectiveness of our approaches.

## References

- [1] Momin Abbas, Quan Xiao, Lisha Chen, Pin-Yu Chen, and Tianyi Chen. Sharp-maml: Sharpness-aware model-agnostic meta learning. In *International Conference on Machine Learning, ICML*, pages 10–32, 2022.
- [2] Maksym Andriushchenko and Nicolas Flammarion. Towards understanding sharpness-aware minimization. In *International Conference on Machine Learning, ICML*, Proceedings of Machine Learning Research, pages 639–668. PMLR, 2022.
- [3] Manoj Ghuhana Arivazhagan, Vinay Aggarwal, Aaditya Kumar Singh, and Sunav Choudhary. Federated learning with personalization layers. *arXiv preprint arXiv:1912.00818*, 2019.
- [4] Enrique Tomás Martínez Beltrán, Mario Quiles Pérez, Pedro Miguel Sánchez Sánchez, Sergio López Bernal, G r me Bovet, Manuel Gil P rez, Gregorio Mart nez P rez, and Alberto Huer-tas Celdr n. Decentralized federated learning: Fundamentals, state-of-the-art, frameworks, trends, and challenges. *arXiv preprint arXiv:2211.08413*, 2022.
- [5] Michael Blot, David Picard, Matthieu Cord, and Nicolas Thome. Gossip training for deep learning. *arXiv preprint arXiv:1611.09726*, 2016.
- [6] L on Bottou, Frank E Curtis, and Jorge Nocedal. Optimization methods for large-scale machine learning. *Siam Review*, 60(2):223–311, 2018.
- [7] Debora Caldarola, Barbara Caputo, and Marco Ciccone. Improving generalization in federated learning by seeking flat minima. *CoRR*, abs/2203.11834, 2022.
- [8] Hong-You Chen and Wei-Lun Chao. On bridging generic and personalized federated learning for image classification. *arXiv preprint arXiv:2107.00778*, 2021.
- [9] Liam Collins, Hamed Hassani, Aryan Mokhtari, and Sanjay Shakkottai. Exploiting shared representations for personalized federated learning. In *International Conference on Machine Learning*, pages 2089–2099. PMLR, 2021.
- [10] Rong Dai, Li Shen, Fengxiang He, Xinmei Tian, and Dacheng Tao. Dispfl: Towards communication-efficient personalized federated learning via decentralized sparse training. In *International Conference on Machine Learning, ICML*, Proceedings of Machine Learning Research, pages 4587–4604. PMLR, 2022.
- [11] Rong Dai, Li Shen, Fengxiang He, Xinmei Tian, and Dacheng Tao. Dispfl: Towards communication-efficient personalized federated learning via decentralized sparse training. *arXiv preprint arXiv:2206.00187*, 2022.
- [12] Yuyang Deng, Mohammad Mahdi Kamani, and Mehrdad Mahdavi. Adaptive personalized federated learning. *arXiv preprint arXiv:2003.13461*, 2020.
- [13] Enmao Diao, Jie Ding, and Vahid Tarokh. Heterofl: Computation and communication efficient federated learning for heterogeneous clients. *arXiv preprint arXiv:2010.01264*, 2020.
- [14] Jiawei Du, Hanshu Yan, Jiashi Feng, Joey Tianyi Zhou, Liangli Zhen, Rick Siow Mong Goh, and Vincent Tan. Efficient sharpness-aware minimization for improved training of neural networks. In *International Conference on Learning Representations*, 2021.

- [15] Pierre Foret, Ariel Kleiner, Hossein Mobahi, and Behnam Neyshabur. Sharpness-aware minimization for efficiently improving generalization. In *International Conference on Learning Representations*, 2021.
- [16] Saeed Ghadimi and Guanghui Lan. Stochastic first-and zeroth-order methods for nonconvex stochastic programming. *SIAM Journal on Optimization*, 23(4):2341–2368, 2013.
- [17] Avishek Ghosh, Jichan Chung, Dong Yin, and Kannan Ramchandran. An efficient framework for clustered federated learning. *Advances in Neural Information Processing Systems*, 33: 19586–19597, 2020.
- [18] Abolfazl Hashemi, Anish Acharya, Rudrajit Das, Haris Vikalo, Sujay Sanghavi, and Inderjit Dhillon. On the benefits of multiple gossip steps in communication-constrained decentralized federated learning. *IEEE Transactions on Parallel and Distributed Systems, TPDS*, pages 2727–2739, 2022.
- [19] Chaoyang He, Murali Annavaram, and Salman Avestimehr. Group knowledge transfer: Federated learning of large cnns at the edge. *Advances in Neural Information Processing Systems*, 33: 14068–14080, 2020.
- [20] Kaiming He, Xiangyu Zhang, Shaoqing Ren, and Jian Sun. Deep residual learning for image recognition. In *Proceedings of the IEEE conference on computer vision and pattern recognition*, pages 770–778, 2016.
- [21] Kevin Hsieh, Amar Phanishayee, Onur Mutlu, and Phillip Gibbons. The non-iid data quagmire of decentralized machine learning. In *International Conference on Machine Learning*, pages 4387–4398. PMLR, 2020.
- [22] Tzu-Ming Harry Hsu, Hang Qi, and Matthew Brown. Measuring the effects of non-identical data distribution for federated visual classification. *arXiv preprint arXiv:1909.06335*, 2019.
- [23] Tiansheng Huang, Shiwei Liu, Li Shen, Fengxiang He, Weiwei Lin, and Dacheng Tao. Achieving personalized federated learning with sparse local models. *arXiv preprint arXiv:2201.11380*, 2022.
- [24] Yutao Huang, Lingyang Chu, Zirui Zhou, Lanjun Wang, Jiangchuan Liu, Jian Pei, and Yong Zhang. Personalized cross-silo federated learning on non-iid data. In *Proceedings of the AAAI Conference on Artificial Intelligence*, volume 35, pages 7865–7873, 2021.
- [25] Zhuo Huang, Xiaobo Xia, Li Shen, Jun Yu, Chen Gong, Bo Han, and Tongliang Liu. Robust generalization against corruptions via worst-case sharpness minimization.
- [26] Eunjeong Jeong and Marios Kountouris. Personalized decentralized federated learning with knowledge distillation. *arXiv preprint arXiv:2302.12156*, 2023.
- [27] Peter Kairouz, H Brendan McMahan, Brendan Avent, Aurélien Bellet, Mehdi Bennis, Arjun Nitin Bhagoji, Kallista Bonawitz, Zachary Charles, Graham Cormode, Rachel Cummings, et al. Advances and open problems in federated learning. *Foundations and Trends in Machine Learning*, pages 1–210, 2021.
- [28] Jiawen Kang, Dongdong Ye, Jiangtian Nie, Jiang Xiao, Xianjun Deng, Siming Wang, Zehui Xiong, Rong Yu, and Dusit Niyato. Blockchain-based federated learning for industrial metaverses: Incentive scheme with optimal aoi. In *2022 IEEE International Conference on Blockchain (Blockchain)*, pages 71–78. IEEE, 2022.
- [29] Anastasia Koloskova, Sebastian Stich, and Martin Jaggi. Decentralized stochastic optimization and gossip algorithms with compressed communication. In *International Conference on Machine Learning*, pages 3478–3487. PMLR, 2019.
- [30] Alex Krizhevsky, Geoffrey Hinton, et al. Learning multiple layers of features from tiny images. 2009.
- [31] Jungmin Kwon, Jeongseop Kim, Hyunseo Park, and In Kwon Choi. Asam: Adaptive sharpness-aware minimization for scale-invariant learning of deep neural networks. In *International Conference on Machine Learning*, pages 5905–5914. PMLR, 2021.

- [32] Ya Le and Xuan Yang. Tiny imagenet visual recognition challenge. *CS 231N*, 7(7):3, 2015.
- [33] Boyue Li, Shicong Cen, Yuxin Chen, and Yuejie Chi. Communication-efficient distributed optimization in networks with gradient tracking and variance reduction. *Journal of Machine Learning Research, JMLR*, pages 180:1–180:51, 2020.
- [34] Daliang Li and Junpu Wang. Fedmd: Heterogenous federated learning via model distillation. *arXiv preprint arXiv:1910.03581*, 2019.
- [35] Jun Li, Yumeng Shao, Kang Wei, Ming Ding, Chuan Ma, Long Shi, Zhu Han, and H. Vincent Poor. Blockchain assisted decentralized federated learning (blade-fl): Performance analysis and resource allocation. *IEEE Transactions on Parallel and Distributed Systems*, 33(10):2401–2415, 2022. doi: 10.1109/TPDS.2021.3138848.
- [36] Shuangtong Li, Tianyi Zhou, Xinmei Tian, and Dacheng Tao. Learning to collaborate in decentralized learning of personalized models. In *Proceedings of the IEEE/CVF Conference on Computer Vision and Pattern Recognition*, pages 9766–9775, 2022.
- [37] Tian Li, Anit Kumar Sahu, Ameet Talwalkar, and Virginia Smith. Federated learning: Challenges, methods, and future directions. *IEEE Signal Processing Magazine*, pages 50–60, 2020.
- [38] Tian Li, Shengyuan Hu, Ahmad Beirami, and Virginia Smith. Ditto: Fair and robust federated learning through personalization. In *International Conference on Machine Learning*, pages 6357–6368. PMLR, 2021.
- [39] Xiangru Lian, Ce Zhang, Huan Zhang, Cho-Jui Hsieh, Wei Zhang, and Ji Liu. Can decentralized algorithms outperform centralized algorithms? a case study for decentralized parallel stochastic gradient descent. In *Advances in Neural Information Processing Systems*, pages 5330–5340, 2017.
- [40] Tao Lin, Lingjing Kong, Sebastian U Stich, and Martin Jaggi. Ensemble distillation for robust model fusion in federated learning. *Advances in Neural Information Processing Systems*, 33: 2351–2363, 2020.
- [41] Tao Lin, Sai Praneeth Karimireddy, Sebastian U Stich, and Martin Jaggi. Quasi-global momentum: Accelerating decentralized deep learning on heterogeneous data. *arXiv preprint arXiv:2102.04761*, 2021.
- [42] Yong Liu, Siqi Mai, Xiangning Chen, Cho-Jui Hsieh, and Yang You. Towards efficient and scalable sharpness-aware minimization. In *Proceedings of the IEEE/CVF Conference on Computer Vision and Pattern Recognition*, pages 12360–12370, 2022.
- [43] Michael McCloskey and Neal J Cohen. Catastrophic interference in connectionist networks: The sequential learning problem. In *Psychology of learning and motivation*, volume 24, pages 109–165. Elsevier, 1989.
- [44] Brendan McMahan, Eider Moore, Daniel Ramage, Seth Hampson, and Blaise Aguera y Arcas. Communication-efficient learning of deep networks from decentralized data. In *Artificial intelligence and statistics*, pages 1273–1282. PMLR, 2017.
- [45] Peng Mi, Li Shen, Tianhe Ren, Yiyi Zhou, Xiaoshuai Sun, Rongrong Ji, and Dacheng Tao. Make sharpness-aware minimization stronger: A sparsified perturbation approach. In Alice H. Oh, Alekh Agarwal, Danielle Belgrave, and Kyunghyun Cho, editors, *Advances in Neural Information Processing Systems*, 2022. URL [https://openreview.net/forum?id=88\\_wNI6ZBDZ](https://openreview.net/forum?id=88_wNI6ZBDZ).
- [46] TV Nguyen, MA Dakka, SM Diakiw, MD VerMilyea, M Perugini, JMM Hall, and D Perugini. A novel decentralized federated learning approach to train on globally distributed, poor quality, and protected private medical data. *Scientific Reports*, 12(1):8888, 2022.
- [47] Jaehoon Oh, Sangmook Kim, and Se-Young Yun. Fedbabu: Towards enhanced representation for federated image classification. *arXiv preprint arXiv:2106.06042*, 2021.

- [48] Krishna Pillutla, Kshitiz Malik, Abdel-Rahman Mohamed, Mike Rabbat, Maziar Sanjabi, and Lin Xiao. Federated learning with partial model personalization. In *International Conference on Machine Learning*, pages 17716–17758. PMLR, 2022.
- [49] Zhe Qu, Xingyu Li, Rui Duan, Yao Liu, Bo Tang, and Zhuo Lu. Generalized federated learning via sharpness aware minimization. In *International Conference on Machine Learning, ICML*, pages 18250–18280, 2022.
- [50] Sashank J. Reddi, Zachary Charles, Manzil Zaheer, Zachary Garrett, Keith Rush, Jakub Konečný, Sanjiv Kumar, and Hugh Brendan McMahan. Adaptive federated optimization. In *International Conference on Learning Representations*, 2021. URL <https://openreview.net/forum?id=LkFG31B13U5>.
- [51] Herbert Robbins and Sutton Monro. A stochastic approximation method. *The annals of mathematical statistics*, pages 400–407, 1951.
- [52] Abhijit Guha Roy, Shayan Siddiqui, Sebastian Pölsterl, Nassir Navab, and Christian Wachinger. Braintorrent: A peer-to-peer environment for decentralized federated learning. *arXiv preprint arXiv:1905.06731*, 2019.
- [53] Abdurakhmon Sadiev, Ekaterina Borodich, Aleksandr Beznosikov, Darina Dvinskikh, Saveliy Chezhegov, Rachael Tappenden, Martin Takáč, and Alexander Gasnikov. Decentralized personalized federated learning: Lower bounds and optimal algorithm for all personalization modes. *EURO Journal on Computational Optimization*, 10:100041, 2022.
- [54] Felix Sattler, Klaus-Robert Müller, and Wojciech Samek. Clustered federated learning: Model-agnostic distributed multitask optimization under privacy constraints. *IEEE transactions on neural networks and learning systems*, 32(8):3710–3722, 2020.
- [55] Yifan Shi, Yingqi Liu, Kang Wei, Li Shen, Xueqian Wang, and Dacheng Tao. Make landscape flatter in differentially private federated learning. *arXiv preprint arXiv:2303.11242*, 2023.
- [56] Yifan Shi, Li Shen, Kang Wei, Yan Sun, Bo Yuan, Xueqian Wang, and Dacheng Tao. Improving the model consistency of decentralized federated learning. *arXiv preprint arXiv:2302.04083*, 2023.
- [57] Yifan Shi, Kang Wei, Li Shen, Yingqi Liu, Xueqian Wang, Bo Yuan, and Dacheng Tao. Towards the flatter landscape and better generalization in federated learning under client-level differential privacy. *arXiv preprint arXiv:2305.00873*, 2023.
- [58] Neta Shoham, Tomer Avidor, Aviv Keren, Nadav Israel, Daniel Benditkis, Liron Mor-Yosef, and Itai Zeitak. Overcoming forgetting in federated learning on non-iid data. *arXiv preprint arXiv:1910.07796*, 2019.
- [59] Sebastian Urban Stich. Local sgd converges fast and communicates little. In *ICLR 2019-International Conference on Learning Representations*, number CONF, 2019.
- [60] Hao Sun, Li Shen, Qihuang Zhong, Liang Ding, Shixiang Chen, Jingwei Sun, Jing Li, Guangzhong Sun, and Dacheng Tao. Adasam: Boosting sharpness-aware minimization with adaptive learning rate and momentum for training deep neural networks. *arXiv preprint arXiv:2303.00565*, 2023.
- [61] Tao Sun, Dongsheng Li, and Bao Wang. Decentralized federated averaging. *IEEE Transactions on Pattern Analysis and Machine Intelligence*, 2022.
- [62] Yan Sun, Li Shen, Tiansheng Huang, Liang Ding, and Dacheng Tao. Fedsspeed: Larger local interval, less communication round, and higher generalization accuracy. In *International Conference on Learning Representations*.
- [63] Alysa Ziyang Tan, Han Yu, Lizhen Cui, and Qiang Yang. Towards personalized federated learning. *IEEE Transactions on Neural Networks and Learning Systems*, 2022.
- [64] Lun Wang, Yang Xu, Hongli Xu, Min Chen, and Liusheng Huang. Accelerating decentralized federated learning in heterogeneous edge computing. *IEEE Transactions on Mobile Computing*, 2022.

- [65] Yuntao Wang, Zhou Su, Ning Zhang, and Abderrahim Benslimane. Learning in the air: Secure federated learning for uav-assisted crowdsensing. *IEEE Transactions on network science and engineering*, 8(2):1055–1069, 2020.
- [66] Yuxin Wu and Kaiming He. Group normalization. In *Proceedings of the European conference on computer vision (ECCV)*, pages 3–19, 2018.
- [67] Haibo Yang, Minghong Fang, and Jia Liu. Achieving linear speedup with partial worker participation in non-IID federated learning. In *International Conference on Learning Representations*, 2021.
- [68] Haishan Ye and Tong Zhang. Deepca: Decentralized exact pca with linear convergence rate. *J. Mach. Learn. Res.*, 22(238):1–27, 2021.
- [69] Haishan Ye, Ziang Zhou, Luo Luo, and Tong Zhang. Decentralized accelerated proximal gradient descent. *Advances in Neural Information Processing Systems*, 33:18308–18317, 2020.
- [70] Zhengxin Yu, Jia Hu, Geyong Min, Han Xu, and Jed Mills. Proactive content caching for internet-of-vehicles based on peer-to-peer federated learning. In *2020 IEEE 26th International Conference on Parallel and Distributed Systems (ICPADS)*, pages 601–608. IEEE, 2020.
- [71] Michael Zhang, Karan Sapra, Sanja Fidler, Serena Yeung, and Jose M Alvarez. Personalized federated learning with first order model optimization. *arXiv preprint arXiv:2012.08565*, 2020.
- [72] Yang Zhao, Hao Zhang, and Xiuyuan Hu. Penalizing gradient norm for efficiently improving generalization in deep learning. In *International Conference on Machine Learning, ICML*, pages 26982–26992. PMLR, 2022.
- [73] Qihuang Zhong, Liang Ding, Li Shen, Peng Mi, Juhua Liu, Bo Du, and Dacheng Tao. Improving sharpness-aware minimization with fisher mask for better generalization on language models. *arXiv preprint arXiv:2210.05497*, 2022.
- [74] Tongtian Zhu, Fengxiang He, Lan Zhang, Zhengyang Niu, Mingli Song, and Dacheng Tao. Topology-aware generalization of decentralized sgd. In *International Conference on Machine Learning, ICML*, pages 27479–27503. PMLR, 2022.

---

## Supplementary Material for “Towards More Suitable Personalization in Federated Learning via Decentralized Partial Model Training”

---

In this part, we provide the supplementary materials including more introduction to the related works, experimental details and results, and the proof of the main theorem.

- **Appendix A:** More details in the related works.
- **Appendix B:** More details in the experiments.
- **Appendix C:** Proof of the theoretical analysis.

### A More Details in the Related Works

**Decentralized/Distributed Training.** By combining SGD and gossip, early work achieved decentralized training and convergence of the model in [5]. D-PSGD [39] is the classic decentralized parallel SGD method. FastMix [69] investigates the advantage of increasing the frequency of local communications within a network topology, in which the optimal computational complexity and near-optimal communication complexity are established. DeEPCA [68] integrates FastMix into a decentralized PCA algorithm to accelerate the training process. DeLi-CoCo [18] performs multiple compression gossip steps in each iteration for fast convergence with arbitrary communication compression. Network-DANE [33] uses multiple gossip steps and generalizes DANE to decentralized scenarios. The work in [41] modifies the momentum term of decentralized SGD (DSGD) to be adaptive to heterogeneous data, while the work in [21] replaces batch norm with layer norm. [36] dynamically updates the mixing weights based on meta-learning and learns a sparse topology to reduce communication costs. The work in [74] provides the topology-aware generalization analysis for DSGD, they explore the impact of various communication topologies on the generalizability.

**Sharpness Aware Minimization (SAM).** SAM [15] is an effective optimizer for training deep learning (DL) models, which leverages the flatness geometry of the loss landscape to improve model generalization ability. Recently, the work in [2] studies the properties of SAM and provides convergence results of SAM for non-convex objectives. As a powerful optimizer, SAM and its variants have been applied to various DL tasks [72; 31; 14; 42; 1; 45; 73; 25] and FL tasks [49; 7; 62; 60; 56; 57; 55]. For instance, the works in [49], [62], and [7] integrate SAM to improve the generalization, and thus mitigate the distribution shift and achieve a new SOTA performance for FL.

### B More Details in the Experiment

In this section, we provide more details of our experiments and more extensive experimental results to compare the performance of the proposed DFedAlt and DFedSalt against other baselines.

#### B.1 Datasets and Data Partition

Table 4: The details on the CIFAR-10 and CIFAR-100 datasets.

Dataset	Training Data	Test Data	Class	Size
CIFAR-10	50,000	10,000	10	3×32×32
CIFAR-100	50,000	10,000	100	3×32×32
Tiny-ImageNet	100,000	10,000	200	3×64×64

CIFAR-10/100 and Tiny-ImageNet are three basic datasets in the computer vision study. As shown in Table 4, they are all colorful images with different classes and different resolutions. We use two non-IID partition methods to split the training data in our implementation. One is based on Dirichlet



distribution on the label ratios to ensure data heterogeneity among clients, where a smaller  $\alpha$  means higher heterogeneity. Another assigns each client a limited number of categories, called Pathological distribution, where fewer categories mean higher heterogeneity. The distribution of the test datasets is the same as in training datasets. We run 500 communication rounds for CIFAR-10, CIFAR-100, and 300 rounds for Tiny-ImageNet.

## B.2 More Details about Baselines

**Local** is the simplest method for personalized learning. It only trains the personalized model on the local data and does not communicate with other clients. For the fair competition, we train 5 epochs locally in each round.

**FedAvg**[44] is the most commonly discussed method in FL. It selects some clients to perform local training on each dataset and then aggregates the trained local models to update the global model. Actually, the local model in FedAvg is also the comparable personalized model for each client.

**FedPer**[3] proposes a base + personalized layer approach for PFL to combat the ill effects of statistical heterogeneity. We set the linear layer as the personalized layer and the rest model as the base layer. It follows FedAvg’s training paradigm but only passes the base layer to the server and keeps the personalized layer locally.

**FedRep**[9] also proposes a body(base layer) + head(personalized layer) framework like FedPer, but it fixes one part when updating the other. We follow the official implementation<sup>3</sup> to train the head for 10 epochs with the body fixed, and then train the body for 5 epochs with the head fixed.

**FedBABU**[47] is also a model split method that achieves good personalization via fine-tuning from a good shared representation base layer. Different from FedPer and FedRep, FedBABU only updates the base layer with the personalized layer fixed and finally fine-tunes the whole model. Following the official implementation<sup>4</sup>, it fine-tunes 5 times in our experiments.

**Fed-RoD**[8] explicitly decouples a model’s dual duties with two prediction tasks—generic optimization and personalized optimization and utilizes a hyper network to connect the generic model and the personalized model. Each client first updates the generic model with balanced risk minimization then updates the personalized model with empirical risk minimization.

**Ditto**[38] achieves personalization via a trade-off between the global model and local objectives. It totally trains two models on the local datasets, one for the global model (similarly aggregated as in FedAvg) with its local empirical risk, and one for the personal model (kept locally) with both empirical risk and the proximal term towards the global model. We set the regularization parameters  $\lambda$  as 0.75.

**DFedAvgM**[61] is the decentralized FedAvg with momentum, in which clients only connect with their neighbors by an undirected graph. For each client, it first initials the local model with the received models then updates it on the local datasets with a local stochastic gradient.

**DFedSAM**[56] leverages gradient perturbation to generate local flat models via Sharpness Aware Minimization (SAM). The communication framework between neighbors is the same as DFedAvgM, but the local update is performed by the SAM optimizer. We set the perturbation radius  $\rho = 0.01$  in our experiments followed by [56].

**Dis-PFL**[11] employs personalized sparse masks to customize sparse local models in the PFL setting. Each client first initials the local model with the personalized sparse masks and updates it with empirical risk. Then filter out the parameter weights that have little influence on the gradient through cosine annealing pruning to obtain a new mask. Following the official implementation<sup>5</sup>, the sparsity of the local model is set to 0.5 for all clients.

## B.3 More Experiments Results on Tiny Imagenet

**Comparison with the baselines.** In Table 5 and Figure 7, we compare DFedAlt and DFedSalt with other baselines on the Tiny-ImageNet with different data distributions. The comparison shows that

<sup>3</sup><https://github.com/lgcollins/FedRep>

<sup>4</sup><https://github.com/jhoon-oh/FedBABU>

<sup>5</sup><https://github.com/rong-dai/DisPFL>

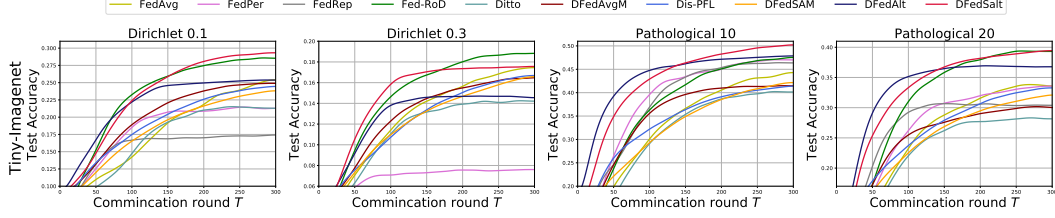


Figure 7: Test accuracy on Tiny-ImageNet with heterogeneous data partitions.

Table 5: Test accuracy (%) on Tiny-ImageNet in both Dirichlet and Pathological distribution settings on Tiny-ImageNet.

Algorithm	Tiny-ImageNet			
	Dirichlet		Pathological	
	$\alpha = 0.1$	$\alpha = 0.3$	$c = 10$	$c = 20$
Local	12.13 $\pm$ .13	5.42 $\pm$ .21	28.49 $\pm$ .16	16.72 $\pm$ .34
FedAvg	25.55 $\pm$ .02	17.58 $\pm$ .25	44.56 $\pm$ .39	34.10 $\pm$ .59
FedPer	21.64 $\pm$ .72	7.71 $\pm$ .08	47.35 $\pm$ .03	33.68 $\pm$ .33
FedRep	17.54 $\pm$ .79	5.78 $\pm$ .05	46.76 $\pm$ .73	31.15 $\pm$ .54
FedBABU	27.40 $\pm$ .08	<b>19.73</b> $\pm$ .06	46.53 $\pm$ .20	38.68 $\pm$ .31
Fed-RoD	29.03 $\pm$ .55	19.25 $\pm$ .45	48.01 $\pm$ .40	39.28 $\pm$ .58
Ditto	21.71 $\pm$ .66	14.47 $\pm$ .14	40.65 $\pm$ .15	28.74 $\pm$ .38
DFedAvgM	25.29 $\pm$ .26	17.07 $\pm$ .17	42.80 $\pm$ .43	30.58 $\pm$ .51
Dis-PFL	24.71 $\pm$ .18	16.94 $\pm$ .36	41.93 $\pm$ .12	33.57 $\pm$ .62
DFedSAM	24.18 $\pm$ .32	16.92 $\pm$ .19	42.87 $\pm$ .31	32.61 $\pm$ .14
DFedAlt	25.71 $\pm$ .20	14.94 $\pm$ .44	49.16 $\pm$ .19	37.25 $\pm$ .27
DFedSalt	<b>29.70</b> $\pm$ .47	17.81 $\pm$ .35	<b>50.79</b> $\pm$ .28	<b>39.44</b> $\pm$ .40

the proposed methods have a competitive performance, especially under higher heterogeneity, e.g. for Dirichlet-0.1 and Pathological-10. Specifically in the Dirichlet-0.1 setting, DFedSalt achieves 29.70%, at least 0.67% improvement from the CFL methods, while DFedSalt and DFedAlt are 1.15% and 2.78% ahead of the other baselines in Pathological-10 setting. The original intention of our design is to build a great personalized model by focusing on local training and exchanging the feature extraction capabilities with neighbors via decentralized partial model training. So when the heterogeneity increases, our algorithms have a significant improvement.

Table 6: The required communication rounds when achieving the target accuracy (%) on Tiny-ImageNet.

Algorithm	Tiny-ImageNet							
	Dirichlet-0.1		Dirichlet-0.3		Pathological-10		Pathological-20	
	acc@20	speedup	acc@14	speedup	acc@40	speedup	acc@30	speedup
FedAvg	160	1.11 $\times$	144	1.47 $\times$	192	1.36 $\times$	172	1.50 $\times$
FedPer	123	1.45 $\times$	-	-	103	2.53 $\times$	134	1.93 $\times$
FedRep	-	-	-	-	116	2.25 $\times$	117	2.21 $\times$
FedBABU	156	1.14 $\times$	174	1.22 $\times$	178	1.47 $\times$	181	1.43 $\times$
Fed-RoD	<b>72</b>	<b>2.47 <math>\times</math></b>	92	2.30 $\times$	132	1.98 $\times$	95	2.72 $\times$
Ditto	178	1.00 $\times$	212	1.00 $\times$	261	1.00 $\times$	-	-
DFedAvgM	115	1.55 $\times$	136	1.56 $\times$	160	1.63 $\times$	258	1.00 $\times$
Dis-PFL	143	1.24 $\times$	166	1.28 $\times$	227	1.15 $\times$	188	1.37 $\times$
DFedSAM	158	1.13 $\times$	174	1.22 $\times$	229	1.14 $\times$	214	1.21 $\times$
DFedAlt	74	2.41 $\times$	108	1.96 $\times$	<b>54</b>	<b>4.83 <math>\times</math></b>	<b>53</b>	<b>4.87 <math>\times</math></b>
DFedSalt	82	2.17 $\times$	<b>78</b>	<b>2.72 <math>\times</math></b>	70	3.73 $\times$	73	3.53 $\times$

**Convergence speed.** We show the convergence speed of DFedAlt and DFedSalt in Table 6 by reporting the number of rounds required to achieve the target personalized accuracy (acc@) on Tiny-ImageNet. For each setting, we set the algorithm that takes the most rounds to reach the target accuracy as “1.00 $\times$ ”, and find that the proposed DFedAlt and DFedSalt achieve the fastest convergence speed on average (3.51 $\times$  and 3.04 $\times$  on average) among the SOTA PFL algorithms. Local training in PFL consistently pursues empirical risk minimization on the local datasets, which can efficiently train the personalized model fitting the local distribution. Also, the alternate updating mode will bring a comparable gain to the convergence speed from the difference between DFedAlt

and DFedAvgM. Thus, our methods can efficiently train the personalized model, especially on the higher heterogeneity.

## C Proof of Theoretical Analysis

### C.1 Preliminary Lemmas

**Lemma 1** (Lemma 4, [39]). *For any  $t \in \mathbb{Z}^+$ , the mixing matrix  $\mathbf{W} \in \mathbb{R}^m$  satisfies  $\|\mathbf{W}^t - \mathbf{P}\|_{\text{op}} \leq \lambda^t$ , where  $\lambda := \max\{|\lambda_2|, |\lambda_m(W)|\}$  and for a matrix  $\mathbf{A}$ , we denote its spectral norm as  $\|\mathbf{A}\|_{\text{op}}$ . Furthermore,  $\mathbf{1} := [1, 1, \dots, 1]^\top \in \mathbb{R}^m$  and*

$$\mathbf{P} := \frac{\mathbf{1}\mathbf{1}^\top}{m} \in \mathbb{R}^{m \times m}.$$

**Lemma 2** (Lemma 23, [48]). *Consider  $F$  which is  $L$ -smooth and fix a  $v^0 \in \mathbb{R}^d$ . Define the sequence  $(v^k)$  of iterates produced by stochastic gradient descent with a fixed learning rate  $\eta_v \leq 1/(2K_v L_v)$  starting from  $v^0$ , we have the bound*

$$\mathbb{E}\|v^{K_v-1} - v^0\|^2 \leq 16\eta_v^2 K_v^2 \mathbb{E}\|\nabla F(v^0)\|^2 + 8\eta_v^2 K_v^2 \sigma_v^2.$$

**Lemma 3** (Local update for shared model  $u_i$  in DFedAlt). *Assume that assumptions 1-3 hold, for all clients  $i \in \{1, 2, \dots, m\}$  and local iteration steps  $k \in \{0, 1, \dots, K_u - 1\}$ , we can get*

$$\frac{1}{m} \sum_{i=1}^m \mathbb{E}\|u_i^{t,k} - u_i^t\|^2 \leq 18\eta_u^2 K_u^2 \left( \sigma_u^2 + \delta^2 + \frac{1}{m} \sum_{i=1}^m \mathbb{E}\|\nabla_u F(u_i^t, V^{t+1})\|^2 \right).$$

*Proof.*

$$\begin{aligned} \frac{1}{m} \sum_{i=1}^m \mathbb{E}\|u_i^{t,k+1} - u_i^t\|^2 &\leq \frac{1}{m} \sum_{i=1}^m \mathbb{E}\left\|u_i^{t,k} - \eta_u \nabla_u F_i(u_i^{t,k}, v_i^{t+1}; \xi_i) - u_i^t\right\|^2 \\ &\leq \frac{1}{m} \sum_{i=1}^m \mathbb{E}\left\|u_i^{t,k} - u_i^t - \eta_u \left( \nabla_u F_i(u_i^{t,k}, v_i^{t+1}; \xi_i) - \nabla_u F_i(u_i^{t,k}, v_i^{t+1}) + \nabla_u F_i(u_i^{t,k}, v_i^{t+1}) \right. \right. \\ &\quad \left. \left. - \nabla_u F_i(u_i^t, V^{t+1}) + \nabla_u F_i(u_i^t, V^{t+1}) \right)\right\|^2 \\ &\leq \text{I} + \text{II}. \end{aligned}$$

Where

$$\text{I} = \left(1 + \frac{1}{2K_u - 1}\right) \frac{1}{m} \sum_{i=1}^m \mathbb{E}\|u_i^{t,k} - u_i^t\|^2,$$

and

$$\text{II} = \frac{2K_u^2 \eta_u^2}{m} \sum_{i=1}^m \mathbb{E}\left\| \nabla_u F_i(u_i^{t,k}, v_i^{t+1}; \xi_i) - \nabla_u F_i(u_i^{t,k}, v_i^{t+1}) + \nabla_u F_i(u_i^{t,k}, v_i^{t+1}) - \nabla_u F(u_i^t, V^{t+1}) + \nabla_u F(u_i^t, V^{t+1}) \right\|^2.$$

For II, we use assumptions 2-3 and generate the following:

$$\text{II} = 6\eta_u^2 K_u \left( \sigma_u^2 + \delta^2 + \frac{1}{m} \sum_{i=1}^m \mathbb{E}\|\nabla_u F(u_i^t, V^{t+1})\|^2 \right).$$

Therefore, the recursion from  $j = 0$  to  $K_u - 1$  can generate:

$$\begin{aligned} \frac{1}{m} \sum_{i=1}^m \mathbb{E}\|u_i^{t,k} - u_i^t\|^2 &\leq \sum_{j=0}^{K_u-1} \left(1 + \frac{1}{2K_u - 1}\right)^j \text{II} \\ &\leq (2K_u - 1) \left[ \left(1 + \frac{1}{2K_u - 1}\right)^{K_u} - 1 \right] \text{II} \\ &\stackrel{a)}{\leq} 3K_u \text{II} \\ &\leq 18\eta_u^2 K_u^2 \left( \sigma_u^2 + \delta^2 + \frac{1}{m} \sum_{i=1}^m \mathbb{E}\|\nabla_u F(u_i^t, V^{t+1})\|^2 \right), \end{aligned}$$

where a) uses  $1 + \frac{1}{2K_u - 1} \leq 2$  and  $(1 + \frac{1}{2K_u - 1})^{2K_u - \frac{1}{2}} \leq \sqrt{5} < \frac{5}{2}$  for any  $K_u \geq 1$ .  $\square$

**Lemma 4** (Local update for shared model  $u_i$  in DFedSalt). *Assume that assumptions 1-3 hold, for all clients  $i \in \{1, 2, \dots, m\}$  and local iteration steps  $k \in \{0, 1, \dots, K_u - 1\}$ , we can get*

$$\frac{1}{m} \sum_{i=1}^m \mathbb{E} \|u_i^{t,k} - u_i^t\|^2 \leq 6\eta_u^2 K_u L_u^2 \rho^2 + 18\eta_u^2 K_u^2 (\sigma_u^2 + \delta^2 + \frac{1}{m} \sum_{i=1}^m \mathbb{E} \|\nabla_u F(u_i^t, V^{t+1})\|^2).$$

*Proof.*

$$\begin{aligned} \frac{1}{m} \sum_{i=1}^m \mathbb{E} \|u_i^{t,k+1} - u_i^t\|^2 &\leq \frac{1}{m} \sum_{i=1}^m \mathbb{E} \|u_i^{t,k} - \eta_u \nabla_u F_i(u_i^{t,k} + \epsilon(u_i^{t,k}), v_i^{t+1}; \xi_i) - u_i^t\|^2 \\ &\leq \frac{1}{m} \sum_{i=1}^m \mathbb{E} \|u_i^{t,k} - u_i^t - \eta_u (\nabla_u F_i(u_i^{t,k} + \epsilon(u_i^{t,k}), v_i^{t+1}; \xi_i) - \nabla_u F_i(u_i^{t,k}, v_i^{t+1}; \xi_i) \\ &\quad + \nabla_u F_i(u_i^{t,k}, v_i^{t+1}; \xi_i) - \nabla_u F_i(u_i^{t,k}, v_i^{t+1}) + \nabla_u F_i(u_i^{t,k}, v_i^{t+1}) \\ &\quad - \nabla_u F_i(u_i^t, V^{t+1}) + \nabla_u F_i(u_i^t, V^{t+1}))\|^2 \\ &\leq \text{I} + \text{II}. \end{aligned}$$

Where

$$\text{I} = (1 + \frac{1}{2K_u - 1}) \frac{1}{m} \sum_{i=1}^m \mathbb{E} \|u_i^{t,k} - u_i^t - \eta_u (\nabla_u F_i(u_i^{t,k} + \epsilon(u_i^{t,k}), v_i^{t+1}; \xi_i) - \nabla_u F_i(u_i^{t,k}, v_i^{t+1}; \xi_i))\|^2,$$

and

$$\text{II} = \frac{2K_u^2 \eta_u^2}{m} \sum_{i=1}^m \mathbb{E} \|\nabla_u F_i(u_i^{t,k}, v_i^{t+1}; \xi_i) - \nabla_u F_i(u_i^{t,k}, v_i^{t+1}) + \nabla_u F_i(u_i^{t,k}, v_i^{t+1}) - \nabla_u F(u_i^t, V^{t+1}) + \nabla_u F(u_i^t, V^{t+1})\|^2.$$

For I, we use assumption 1 and generate the following:

$$\begin{aligned} \text{I} &\leq (1 + \frac{1}{2K_u - 1}) \frac{1}{m} \sum_{i=1}^m \left( \mathbb{E} \|u_i^{t,k} - u_i^t\|^2 + \eta_u^2 L_u^2 \mathbb{E} \left\| \rho \frac{\nabla_u F_i(u_i^{t,k}, v_i^{t+1}; \xi_i)}{\|\nabla_u F_i(u_i^{t,k}, v_i^{t+1}; \xi_i)\|_2} \right\|^2 \right) \\ &\leq (1 + \frac{1}{2K_u - 1}) \left( \frac{1}{m} \sum_{i=1}^m \mathbb{E} \|u_i^{t,k} - u_i^t\|^2 + \eta_u^2 L_u^2 \rho^2 \right). \end{aligned}$$

For II, we use assumption 2-3 and generate the following:

$$\text{II} = 6\eta_u^2 K_u (\sigma_u^2 + \delta^2 + \frac{1}{m} \sum_{i=1}^m \mathbb{E} \|\nabla_u F(u_i^t, V^{t+1})\|^2).$$

Therefore, the recursion from  $j = 0$  to  $K_u - 1$  can generate:

$$\begin{aligned} \frac{1}{m} \sum_{i=1}^m \mathbb{E} \|u_i^{t,k} - u_i^t\|^2 &\leq \sum_{j=0}^{K_u-1} (1 + \frac{1}{2K_u - 1})^j \left[ (1 + \frac{1}{2K_u - 1}) \eta_u^2 L_u^2 \rho^2 + \text{II} \right] \\ &\leq (2K_u - 1) \left[ (1 + \frac{1}{2K_u - 1})^{K_u} - 1 \right] \left( (1 + \frac{1}{2K_u - 1}) \eta_u^2 L_u^2 \rho^2 + \text{II} \right) \\ &\stackrel{a)}{\leq} 3K_u (\text{II} + 2\eta_u^2 L_u^2 \rho^2) \\ &\leq 6\eta_u^2 K_u L_u^2 \rho^2 + 18\eta_u^2 K_u^2 (\sigma_u^2 + \delta^2 + \frac{1}{m} \sum_{i=1}^m \mathbb{E} \|\nabla_u F(u_i^t, V^{t+1})\|^2), \end{aligned}$$

where a) uses  $1 + \frac{1}{2K_u - 1} \leq 2$  and  $(1 + \frac{1}{2K_u - 1})^{2K_u - 1} \leq \sqrt{5} < \frac{5}{2}$  for any  $K_u \geq 1$ .  $\square$

**Lemma 5** (Shared model shift in DFedAlt). *Assume that assumptions 1-3 hold, for all clients  $i \in \{1, 2, \dots, m\}$  and local iteration steps  $k \in \{1, 2, \dots, K_u\}$ , we can get*

$$\frac{1}{m} \sum_{i=1}^m \mathbb{E} \|u_i^t - \bar{u}^t\|^2 \leq \frac{18\eta_u^2 K_u^2}{(1 - \lambda)^2} (\sigma_u^2 + \delta^2 + \frac{1}{m} \sum_{i=1}^m \mathbb{E} \|\nabla_u F(u_i^t, V^{t+1})\|^2).$$

*Proof.* Inspired by Lemma D.2 in [56] and Lemma 4 in [61], according to Lemma 1, we can generate

$$\begin{aligned}
\mathbb{E}\|U^t - \mathbf{P}U^t\|^2 &\leq \mathbb{E}\left\|\sum_{j=0}^{t-1}(\mathbf{P} - \mathbf{W}^{t-1-j})\zeta^j\right\|^2 \\
&\leq \sum_{j=0}^{t-1}\|\mathbf{P} - \mathbf{W}^{t-1-j}\|_{\text{op}}\|\zeta^j\| \\
&\leq \left(\sum_{j=0}^{t-1}\lambda^{t-1-j}\|\zeta^j\|\right)^2 \\
&\leq \mathbb{E}\left(\sum_{j=0}^{t-1}\lambda^{\frac{t-1-j}{2}} \cdot \lambda^{\frac{t-1-j}{2}}\|\zeta^j\|\right)^2 \\
&\leq \left(\sum_{j=0}^{t-1}\lambda^{t-1-j}\right)\left(\sum_{j=0}^{t-1}\lambda^{t-1-j}\mathbb{E}\|\zeta^j\|^2\right),
\end{aligned}$$

where  $U^t = [u_1^t, u_2^t, \dots, u_m^t]^T \in \mathbb{R}^{m \times d}$  and

$$\mathbb{E}\|\zeta^j\|^2 \leq \|\mathbf{W}\|^2 \cdot \mathbb{E}\|U^j - Z^j\|^2 \leq \mathbb{E}\|U^j - Z^j\|^2.$$

Note that  $Z^t = [z_1^t, z_2^t, \dots, z_m^t]^T \in \mathbb{R}^{m \times d}$ . According to Lemma 3, for any  $j$ , we have

$$\mathbb{E}\|U^j - Z^j\|^2 \leq 18\eta_u^2 K_u^2 m \left( \sigma_u^2 + \delta^2 + \frac{1}{m} \sum_{i=1}^m \mathbb{E}\|\nabla_u F(u_i^t, V^{t+1})\|^2 \right).$$

After that,

$$\mathbb{E}\|U^t - \mathbf{P}U^t\|^2 \leq \frac{18\eta_u^2 K_u^2}{(1-\lambda)^2} \left( \sigma_u^2 + \delta^2 + \frac{1}{m} \sum_{i=1}^m \mathbb{E}\|\nabla_u F(u_i^t, V^{t+1})\|^2 \right).$$

The fact is that  $U^t - \mathbf{P}U^t = \begin{pmatrix} u_1^t - \bar{u}^t \\ u_2^t - \bar{u}^t \\ \vdots \\ u_m^t - \bar{u}^t \end{pmatrix}$  is the result needed to prove. □

**Lemma 6** (Shared model shift in DFedSalt). *Assume that assumptions 1-3 hold, for all clients  $i \in \{1, 2, \dots, m\}$  and local iteration steps  $k \in \{1, 2, \dots, K_u\}$ , we can get*

$$\frac{1}{m} \sum_{i=1}^m \mathbb{E}\|u_i^t - \bar{u}^t\|^2 \leq \frac{6\eta_u^2 K_u}{(1-\lambda)^2} \left[ L_u^2 \rho^2 + 3K_u \left( \sigma_u^2 + \delta^2 + \frac{1}{m} \sum_{i=1}^m \mathbb{E}\|\nabla_u F(u_i^t, V^{t+1})\|^2 \right) \right].$$

*Proof.* Based on Lemma 5 and according to Lemma 4, for any  $j$ , we have

$$\mathbb{E}\|U^j - Z^j\|^2 \leq m \left( 6\eta_u^2 K_u L_u^2 \rho^2 + 18\eta_u^2 K_u^2 \left( \sigma_u^2 + \delta^2 + \frac{1}{m} \sum_{i=1}^m \mathbb{E}\|\nabla_u F(u_i^t, V^{t+1})\|^2 \right) \right).$$

After that,

$$\mathbb{E}\|U^t - \mathbf{P}U^t\|^2 \leq \frac{6\eta_u^2 K_u}{(1-\lambda)^2} \left[ L_u^2 \rho^2 + 3K_u \left( \sigma_u^2 + \delta^2 + \frac{1}{m} \sum_{i=1}^m \mathbb{E}\|\nabla_u F(u_i^t, V^{t+1})\|^2 \right) \right].$$

The fact is that  $U^t - \mathbf{P}U^t = \begin{pmatrix} u_1^t - \bar{u}^t \\ u_2^t - \bar{u}^t \\ \vdots \\ u_m^t - \bar{u}^t \end{pmatrix}$  is the result needed to prove. □

## C.2 Proof of Convergence Analysis

**Proof Outline and the Challenge of Dependent Random Variables.** We start with

$$\begin{aligned} F(\bar{u}^{t+1}, V^{t+1}) - F(\bar{u}^t, V^t) &= F(\bar{u}^t, V^{t+1}) - F(\bar{u}^t, V^t) \\ &\quad + F(\bar{u}^{t+1}, V^{t+1}) - F(\bar{u}^t, V^{t+1}). \end{aligned} \quad (5)$$

The first line corresponds to the effect of the  $v$ -step and the second line to the  $u$ -step. The former is

$$\begin{aligned} F(\bar{u}^t, V^{t+1}) - F(\bar{u}^t, V^t) &= \frac{1}{m} \sum_{i=1}^m \mathbb{E} [F_i(\bar{u}^t, v_i^{t+1}) - F_i(\bar{u}^t, v_i^t)] \\ &\leq \frac{1}{m} \sum_{i=1}^m \mathbb{E} \left[ \left\langle \nabla_v F_i(\bar{u}^t, v_i^t), v_i^{t+1} - v_i^t \right\rangle + \frac{L_v}{2} \|v_i^{t+1} - v_i^t\|^2 \right]. \end{aligned} \quad (6)$$

It is easy to handle with standard techniques that rely on the smoothness of  $F(u^t, \cdot)$ . The latter is more challenging. In particular, the smoothness bound for the  $u$ -step gives us

$$F(\bar{u}^{t+1}, V^{t+1}) - F(\bar{u}^t, V^{t+1}) \leq \left\langle \nabla_u F(\bar{u}^t, V^{t+1}), \bar{u}^{t+1} - \bar{u}^t \right\rangle + \frac{L_u}{2} \|\bar{u}^{t+1} - \bar{u}^t\|^2. \quad (7)$$

### C.2.1 Proof of Convergence Analysis for DFedAlt

**Analysis of the  $u$ -Step.**

$$\begin{aligned} \mathbb{E} [F(\bar{u}^{t+1}, V^{t+1}) - F(\bar{u}^t, V^{t+1})] &\leq \left\langle \nabla_u F(\bar{u}^t, V^{t+1}), \bar{u}^{t+1} - \bar{u}^t \right\rangle + \frac{L_u}{2} \mathbb{E} \|\bar{u}^{t+1} - \bar{u}^t\|^2 \\ &\leq \frac{-\eta_u}{m} \sum_{i=1}^m \mathbb{E} \left\langle \nabla_u F(\bar{u}^t, V^{t+1}), \sum_{k=0}^{K_u-1} \nabla_u F(u_i^{t,k}, v_i^{t+1}; \xi_i) \right\rangle + \frac{L_u}{2} \mathbb{E} \|\bar{u}^{t+1} - \bar{u}^t\|^2 \\ &\leq -\eta_u K_u \mathbb{E} [\Delta_{\bar{u}}^t] + \frac{\eta_u}{m} \sum_{i=1}^m \sum_{k=0}^{K_u-1} \mathbb{E} \left\langle \nabla_u F(\bar{u}^t, V^{t+1}), \nabla F(\bar{u}^t, v_i^{t+1}) - \nabla_u F(u_i^{t,k}, v_i^{t+1}; \xi_i) \right\rangle + \frac{L_u}{2} \mathbb{E} \|\bar{u}^{t+1} - \bar{u}^t\|^2 \\ &\stackrel{a)}{\leq} \underbrace{\frac{-\eta_u K_u}{2} \mathbb{E} [\Delta_{\bar{u}}^t] + \frac{\eta_u L_u^2}{2m} \sum_{i=1}^m \sum_{k=0}^{K_u-1} \mathbb{E} \|u_i^{t,k} - \bar{u}^t\|^2}_{\mathcal{T}_{1,u}} + \underbrace{\frac{L_u}{2} \mathbb{E} \|\bar{u}^{t+1} - \bar{u}^t\|^2}_{\mathcal{T}_{2,u}}. \end{aligned} \quad (8)$$

Where a) uses  $\mathbb{E} [\nabla_u F(u_i^{t,k}, v_i^{t+1}; \xi_i)] = \nabla_u F(u_i^{t,k}, v_i^{t+1})$  and  $\langle x, y \rangle \leq \frac{1}{2} \|x\|^2 + \frac{1}{2} \|y\|^2$  for vectors  $x, y$  followed by  $L_u$ -smoothness.

For  $\mathcal{T}_{1,u}$ , we can use Lemma 5.

$$\mathcal{T}_{1,u} \leq \frac{9\eta_u^3 K_u^2 L_u^2}{(1-\lambda)^2} \left[ \sigma_u^2 + \delta^2 + \underbrace{\frac{1}{m} \sum_{i=1}^m \mathbb{E} \|\nabla_u F(u_i^t, V^{t+1})\|^2}_{\mathcal{T}_{3,u}} \right] \quad (9)$$

For  $\mathcal{T}_{3,u}$ ,

$$\begin{aligned} \mathcal{T}_{3,u} &\leq \frac{1}{m} \sum_{i=1}^m \mathbb{E} \|\nabla_u F(u_i^t, V^{t+1}) - \nabla_u F(\bar{u}^t, V^{t+1}) + \nabla_u F(\bar{u}^t, V^{t+1})\|^2 \\ &\leq \frac{2L_u^2}{m} \sum_{i=1}^m \mathbb{E} \|u_i^t - \bar{u}^t\|^2 + \frac{2}{m} \sum_{i=1}^m \mathbb{E} \|\nabla_u F(\bar{u}^t, V^{t+1})\|^2 \\ &\leq \frac{2L_u^2}{m} \sum_{i=1}^m \mathbb{E} \|u_i^t - \bar{u}^t\|^2 + 2\mathbb{E} [\Delta_{\bar{u}}^t], \end{aligned} \quad (10)$$

After that, combining Eq. (9) and (10) and assuming local learning rate  $\eta_u \ll \frac{1-\lambda}{3\sqrt{2K_u L_u}}$ , we can generate

$$\mathcal{T}_{1,u} \leq \frac{9\eta_u^3 K_u^2 L_u^2}{(1-\lambda)^2} \left[ \sigma_u^2 + \delta^2 + 2\mathbb{E}[\Delta_{\bar{u}}^t] \right]. \quad (11)$$

Meanwhile, for  $\mathcal{T}_{2,u}$ ,

$$\begin{aligned} \mathcal{T}_{2,u} &\leq \frac{\eta_u^2 L_u}{2m} \sum_{i=1}^m \sum_{k=0}^{K_u-1} \left\| \nabla_u F(u_i^{t,k}, v_i^{t+1}; \xi_i) - \nabla_u F(u_i^t, v_i^{t+1}) + \nabla_u F(u_i^t, v_i^{t+1}) \right. \\ &\quad \left. - \nabla_u F(u_i^t, V^{t+1}) + \nabla_u F(u_i^t, V^{t+1}) - \nabla_u F(\bar{u}^t, V^{t+1}) + \nabla_u F(\bar{u}^t, V^{t+1}) \right\|^2 \\ &\leq 2\eta_u^2 K_u L_u \left( \sigma_u^2 + \delta^2 + \frac{L_u^2}{m} \sum_{i=1}^m \mathbb{E} \|u_i^t - \bar{u}^t\|^2 + \mathbb{E}[\Delta_{\bar{u}}^t] \right) \\ &\leq 2\eta_u^2 K_u L_u \left( \sigma_u^2 + \delta^2 + \mathbb{E}[\Delta_{\bar{u}}^t] \right) + \underbrace{\frac{2\eta_u^2 K_u L_u^3}{m} \sum_{i=1}^m \mathbb{E} \|u_i^t - \bar{u}^t\|^2}_{\mathcal{T}_{4,u}} \end{aligned} \quad (12)$$

For  $\mathcal{T}_{4,u}$ , we can use Lemma 5.

After that,

$$\begin{aligned} \mathbb{E} \left[ F(\bar{u}^{t+1}, V^{t+1}) - F(\bar{u}^t, V^{t+1}) \right] &\leq \frac{-\eta_u K_u}{2} \mathbb{E}[\Delta_{\bar{u}}^t] + \mathcal{T}_{1,u} + \mathcal{T}_{2,u} \\ &\leq \left( \frac{-\eta_u K_u}{2} + 2\eta_u^2 K_u L_u + \frac{18\eta_u^2 K_u^2 (2 + \eta_u L_u^2)}{(1-\lambda)^2} \right) \mathbb{E}[\Delta_{\bar{u}}^t] \\ &\quad + 2\eta_u^2 K_u L_u (\sigma_u^2 + \delta^2) + \frac{9\eta_u^2 K_u^2 (2 + \eta_u L_u^2)}{(1-\lambda)^2} (\sigma_u^2 + \delta^2). \end{aligned} \quad (13)$$

**Analysis of the  $v$ -Step.**

$$\mathbb{E} \left[ F(\bar{u}^t, V^{t+1}) - F(\bar{u}^t, V^t) \right] \leq \underbrace{\frac{1}{m} \sum_{i=1}^m \mathbb{E} \langle \nabla_v F_i(\bar{u}^t, v_i^t), v_i^{t+1} - v_i^t \rangle}_{\mathcal{T}_{1,v}} + \underbrace{\frac{L_v}{2m} \sum_{i=1}^m \mathbb{E} \|v_i^{t+1} - v_i^t\|^2}_{\mathcal{T}_{2,v}}. \quad (14)$$

For  $\mathcal{T}_{1,v}$ ,

$$\begin{aligned} \mathcal{T}_{1,v} &\leq \frac{1}{m} \sum_{i=1}^m \mathbb{E} \langle \nabla_v F_i(\bar{u}^t, v_i^t) - \nabla_v F_i(u_i^t, v_i^t) + \nabla_v F_i(u_i^t, v_i^t), -\eta_v \sum_{k=0}^{K_v-1} \mathbb{E} \nabla_v F_i(u_i^t, v_i^t; \xi_i) \rangle \\ &\stackrel{a)}{\leq} \frac{-\eta_v K_v}{m} \sum_{i=1}^m \mathbb{E} \|\nabla_v F_i(u_i^t, v_i^t)\|^2 + \frac{1}{m} \sum_{i=1}^m \mathbb{E} \langle \nabla_v F_i(\bar{u}^t, v_i^t) - \nabla_v F_i(u_i^t, v_i^t), v_i^{t+1} - v_i^t \rangle \\ &\stackrel{b)}{\leq} \underbrace{-\eta_v K_v \mathbb{E}[\Delta_v^t]}_{\mathcal{T}_{3,v}} + \underbrace{\frac{L_{vu}^2}{2m} \sum_{i=1}^m \mathbb{E} \|\bar{u}^t - u_i^t\|^2 + \frac{1}{2m} \sum_{i=1}^m \mathbb{E} \|v_i^{t+1} - v_i^t\|^2}_{\frac{1}{L_v} \mathcal{T}_{2,v}}, \end{aligned} \quad (15)$$

where a) and b) is get from the unbiased expectation property of  $\nabla_v F_i(u_i^t, v_i^t; \xi_i)$  and  $\langle x, y \rangle \leq \frac{1}{2}(\|x\|^2 + \|y\|^2)$ , respectively.

For  $\mathcal{T}_{2,v}$ , according to Lemma 2, we have

$$\begin{aligned} \mathcal{T}_{2,v} &\leq \frac{L_v}{2} \left( \frac{16\eta_v^2 K_v^2}{m} \sum_{i=1}^m \mathbb{E} \|\nabla_v F_i(u_i^t, v_i^t)\|^2 + 8\eta_v^2 K_v^2 \sigma_v^2 \right) \\ &\leq 8L_v \eta_v^2 K_v^2 \mathbb{E}[\Delta_v^t] + 4L_v \eta_v^2 K_v^2 \sigma_v^2. \end{aligned} \quad (16)$$



For  $\mathcal{T}_{3,v}$ , according to Eq. (11), we have

$$\frac{L_{vu}^2}{2m} \sum_{i=1}^m \mathbb{E} \|\bar{u}^t - u_i^t\|^2 \leq \frac{L_{vu}^2}{(1-\lambda)^2} \left[ 18\eta_u^2 K_u^2 (\sigma_u^2 + \delta^2 + 2\mathbb{E}[\Delta_{\bar{u}}^t]) \right]. \quad (17)$$

After that, summing Eq. (15), (16), and (17), we have

$$\begin{aligned} \mathbb{E} \left[ F(\bar{u}^t, V^{t+1}) - F(\bar{u}^t, V^t) \right] &\leq \left( -\eta_v K_v + 8\eta_v^2 K_v^2 (L_v + 1) \right) \mathbb{E}[\Delta_v^t] + 4\eta_v^2 K_v^2 \sigma_v^2 (L_v + 1) \\ &\quad + \frac{L_{vu}^2}{(1-\lambda)^2} \left[ 18\eta_u^2 K_u^2 (\sigma_u^2 + \delta^2 + 2\mathbb{E}[\Delta_{\bar{u}}^t]) \right]. \end{aligned} \quad (18)$$

**Obtaining the Final Convergence Bound.**

$$\begin{aligned} \mathbb{E} \left[ F(\bar{u}^{t+1}, V^{t+1}) - F(\bar{u}^t, V^t) \right] &= \mathbb{E} \left[ F(\bar{u}^t, V^{t+1}) - F(\bar{u}^t, V^t) + F(\bar{u}^{t+1}, V^{t+1}) - F(\bar{u}^t, V^{t+1}) \right] \\ &\leq \left( \frac{-\eta_u K_u}{2} + 2\eta_u^2 K_u L_u + \frac{18\eta_u^2 K_u^2 (2 + \eta_u L_u^2)}{(1-\lambda)^2} \right) \mathbb{E}[\Delta_{\bar{u}}^t] \\ &\quad + 2\eta_u^2 K_u L_u (\sigma_u^2 + \delta^2) + \frac{9\eta_u^2 K_u^2 (2 + \eta_u L_u^2)}{(1-\lambda)^2} (\sigma_u^2 + \delta^2) \\ &\quad + \left( -\eta_v K_v + 8\eta_v^2 K_v^2 (L_v + 1) \right) \mathbb{E}[\Delta_v^t] + 4\eta_v^2 K_v^2 \sigma_v^2 (L_v + 1) \\ &\quad + \frac{18\eta_u^2 L_{vu}^2 K_u^2 (\sigma_u^2 + \delta^2 + 2\mathbb{E}[\Delta_{\bar{u}}^t])}{(1-\lambda)^2}. \end{aligned} \quad (19)$$

Summing from  $t = 1$  to  $T$ , assume the local learning rates satisfy  $\eta_u = \mathcal{O}(1/L_u K_u \sqrt{T})$ ,  $\eta_v = \mathcal{O}(1/L_v K_v \sqrt{T})$ ,  $F^*$  is denoted as the minimal value of  $F$ , i.e.,  $F(\bar{u}, V) \geq F^*$  for all  $\bar{u} \in \mathbb{R}^d$ , and  $V = (v_1, \dots, v_m) \in \mathbb{R}^{d_1 + \dots + d_m}$ . We can generate

$$\begin{aligned} \frac{1}{T} \sum_{i=1}^T \left( \frac{1}{L_u} \mathbb{E}[\Delta_{\bar{u}}^t] + \frac{1}{L_v} \mathbb{E}[\Delta_v^t] \right) &\leq \mathcal{O} \left( \frac{F(\bar{u}^1, V^1) - F^*}{\sqrt{T}} + \frac{\sigma_v^2 (L_v + 1)}{L_v^2 \sqrt{T}} \right. \\ &\quad \left. + \frac{L_{vu}^2 (\sigma_u^2 + \delta^2)}{L_u^2 \sqrt{T}} + \frac{\sigma_u^2 + \delta^2}{L_u T (1-\lambda)^2} \right). \end{aligned} \quad (20)$$

Assume that

$$\sigma_1^2 = \frac{\sigma_v^2 (L_v + 1)}{L_v^2} + \frac{L_{vu}^2 (\sigma_u^2 + \delta^2)}{L_u^2} = \frac{\sigma_v^2 (L_v + 1)}{L_v^2} + \frac{\chi^2 L_v (\sigma_u^2 + \delta^2)}{L_u}, \quad \sigma_2^2 = \frac{\sigma_u^2 + \delta^2}{L_u}.$$

Then, we have the final convergence bound:

$$\frac{1}{T} \sum_{i=1}^T \left( \frac{1}{L_u} \mathbb{E}[\Delta_{\bar{u}}^t] + \frac{1}{L_v} \mathbb{E}[\Delta_v^t] \right) \leq \mathcal{O} \left( \frac{F(\bar{u}^1, V^1) - F^*}{\sqrt{T}} + \frac{\sigma_1^2}{\sqrt{T}} + \frac{\sigma_2^2}{T(1-\lambda)^2} \right). \quad (21)$$

### C.2.2 Proof of Convergence Analysis for DFedSalt

#### Analysis of the $u$ -Step.

$$\begin{aligned}
\mathbb{E} \left[ F(\bar{u}^{t+1}, V^{t+1}) - F(\bar{u}^t, V^{t+1}) \right] &\leq \left\langle \nabla_u F(\bar{u}^t, V^{t+1}), \bar{u}^{t+1} - \bar{u}^t \right\rangle + \frac{L_u}{2} \mathbb{E} \|\bar{u}^{t+1} - \bar{u}^t\|^2 \\
&\leq \frac{-\eta_u}{m} \sum_{i=1}^m \mathbb{E} \left\langle \nabla_u F(\bar{u}^t, V^{t+1}), \sum_{k=0}^{K_u-1} \nabla_u F(u_i^{t,k}, v_i^{t+1}; \xi_i) \right\rangle + \frac{L_u}{2} \mathbb{E} \|\bar{u}^{t+1} - \bar{u}^t\|^2 \\
&\leq -\eta_u K_u \mathbb{E}[\Delta_{\bar{u}}^t] + \frac{\eta_u}{m} \sum_{i=1}^m \sum_{k=0}^{K_u-1} \mathbb{E} \left\langle \nabla_u F(\bar{u}^t, V^{t+1}), \nabla F(\bar{u}^t, v_i^{t+1}) - \nabla_u F(u_i^{t,k}, v_i^{t+1}; \xi_i) \right\rangle + \frac{L_u}{2} \mathbb{E} \|\bar{u}^{t+1} - \bar{u}^t\|^2 \\
&\stackrel{a)}{\leq} \underbrace{\frac{-\eta_u K_u}{2} \mathbb{E}[\Delta_{\bar{u}}^t] + \frac{\eta_u L_u^2}{2m} \sum_{i=1}^m \sum_{k=0}^{K_u-1} \mathbb{E} \|u_i^{t,k} - \bar{u}^t\|^2}_{\mathcal{T}_{1,u}} + \underbrace{\frac{L_u}{2} \mathbb{E} \|\bar{u}^{t+1} - \bar{u}^t\|^2}_{\mathcal{T}_{2,u}}.
\end{aligned} \tag{22}$$

Where a) uses  $\mathbb{E} \left[ \nabla_u F(u_i^{t,k}, v_i^{t+1}; \xi_i) \right] = \nabla_u F(\bar{u}^t, v_i^{t+1})$  and  $\langle x, y \rangle \leq \frac{1}{2} \|x\|^2 + \frac{1}{2} \|y\|^2$  for vectors  $x, y$  followed by  $L_u$ -smoothness.

For  $\mathcal{T}_{1,u}$ , we can use Lemma 6.

$$\mathcal{T}_{1,u} \leq \frac{3\eta_u^3 K_u L_u^2}{(1-\lambda)^2} \left[ L_u^2 \rho^2 + 3K_u \left( \sigma_u^2 + \delta^2 + \underbrace{\frac{1}{m} \sum_{i=1}^m \mathbb{E} \|\nabla_u F(u_i^t, V^{t+1})\|^2}_{\mathcal{T}_{3,u}} \right) \right] \tag{23}$$

For  $\mathcal{T}_{3,u}$ ,

$$\begin{aligned}
\mathcal{T}_{3,u} &\leq \frac{1}{m} \sum_{i=1}^m \mathbb{E} \left\| \nabla_u F(u_i^t, V^{t+1}) - \nabla_u F(\bar{u}^t, V^{t+1}) + \nabla_u F(\bar{u}^t, V^{t+1}) \right\|^2 \\
&\leq \frac{2L_u^2}{m} \sum_{i=1}^m \mathbb{E} \|u_i^t - \bar{u}^t\|^2 + \frac{2}{m} \sum_{i=1}^m \mathbb{E} \|\nabla_u F(\bar{u}^t, V^{t+1})\|^2 \\
&\leq \frac{2L_u^2}{m} \sum_{i=1}^m \mathbb{E} \|u_i^t - \bar{u}^t\|^2 + 2\mathbb{E}[\Delta_{\bar{u}}^t],
\end{aligned} \tag{24}$$

After that, combining Eq. (23) and (24) and assuming local learning rate  $\eta_u \ll \frac{1-\lambda}{3\sqrt{2}K_u L_u}$ , we can generate

$$\mathcal{T}_{1,u} \leq \frac{3\eta_u^3 K_u L_u^2}{(1-\lambda)^2} \left[ L_u^2 \rho^2 + 3K_u \left( \sigma_u^2 + \delta^2 + 2\mathbb{E}[\Delta_{\bar{u}}^t] \right) \right]. \tag{25}$$

Meanwhile, for  $\mathcal{T}_{2,u}$ ,

$$\begin{aligned}
\mathcal{T}_{2,u} &\leq \frac{\eta_u^2 L_u}{2m} \sum_{i=1}^m \sum_{k=0}^{K_u-1} \left\| \nabla_u F(u_i^{t,k} + \epsilon(u_i^{t,k}), v_i^{t+1}; \xi_i) - \nabla_u F(u_i^{t,k}, v_i^{t+1}; \xi_i) \right. \\
&\quad \left. + \nabla_u F(u_i^{t,k}, v_i^{t+1}; \xi_i) - \nabla_u F(u_i^t, v_i^{t+1}) + \nabla_u F(u_i^t, v_i^{t+1}) - \nabla_u F(u_i^t, V^{t+1}) + \nabla_u F(u_i^t, V^{t+1}) \right. \\
&\quad \left. - \nabla_u F(\bar{u}^t, V^{t+1}) + \nabla_u F(\bar{u}^t, V^{t+1}) \right\|^2 \\
&\leq \frac{5}{2} \eta_u^2 K_u L_u \left( L_u^2 \rho^2 + \sigma_u^2 + \delta^2 + \frac{L_u^2}{m} \sum_{i=1}^m \mathbb{E} \|u_i^t - \bar{u}^t\|^2 + \mathbb{E}[\Delta_{\bar{u}}^t] \right) \\
&\leq \frac{5}{2} \eta_u^2 K_u L_u \left( L_u^2 \rho^2 + \sigma_u^2 + \delta^2 + \mathbb{E}[\Delta_{\bar{u}}^t] \right) + \underbrace{\frac{5\eta_u^2 K_u L_u^3}{2m} \sum_{i=1}^m \mathbb{E} \|u_i^t - \bar{u}^t\|^2}_{\mathcal{T}_{4,u}}
\end{aligned} \tag{26}$$

For  $\mathcal{T}_{4,u}$ , we can use Lemma 6.

After that,

$$\begin{aligned}
\mathbb{E} \left[ F(\bar{u}^{t+1}, V^{t+1}) - F(\bar{u}^t, V^t) \right] &\leq \frac{-\eta_u K_u}{2} \mathbb{E}[\Delta_u^t] + \mathcal{T}_{1,u} + \mathcal{T}_{2,u} \\
&\leq \left( \frac{-\eta_u K_u}{2} + \frac{5}{2} \eta_u^2 K_u L_u + \frac{18\eta_u^3 K_u^2 L_u^2 (1 + 5\eta_u K_u L_u)}{(1-\lambda)^2} \right) \mathbb{E}[\Delta_u^t] \\
&\quad + \frac{3\eta_u^3 K_u L_u^2}{(1-\lambda)^2} \left[ L_u^2 \rho^2 + 3K_u (\sigma_u^2 + \delta^2) \right] + \frac{5}{2} \eta_u^2 K_u L_u (L_u^2 \rho^2 + \sigma_u^2 + \delta^2) \\
&\quad + \frac{15\eta_u^4 K_u^2 L_u^3}{(1-\lambda)^2} \left[ L_u^2 \rho^2 + 3K_u (\sigma_u^2 + \delta^2) \right].
\end{aligned} \tag{27}$$

**Analysis of the  $v$ -Step.**

$$\mathbb{E} \left[ F(\bar{u}^t, V^{t+1}) - F(\bar{u}^t, V^t) \right] \leq \underbrace{\frac{1}{m} \sum_{i=1}^m \mathbb{E} \left\langle \nabla_v F_i(\bar{u}^t, v_i^t), v_i^{t+1} - v_i^t \right\rangle}_{\mathcal{T}_{1,v}} + \underbrace{\frac{L_v}{2m} \sum_{i=1}^m \mathbb{E} \|v_i^{t+1} - v_i^t\|^2}_{\mathcal{T}_{2,v}}. \tag{28}$$

For  $\mathcal{T}_{1,v}$ ,

$$\begin{aligned}
\mathcal{T}_{1,v} &\leq \frac{1}{m} \sum_{i=1}^m \mathbb{E} \left\langle \nabla_v F_i(\bar{u}^t, v_i^t) - \nabla_v F_i(u_i^t, v_i^t) + \nabla_v F_i(u_i^t, v_i^t), -\eta_v \sum_{k=0}^{K_v-1} \mathbb{E} \nabla_v F_i(u_i^t, v_i^t; \xi_i) \right\rangle \\
&\stackrel{a)}{\leq} \frac{-\eta_v K_v}{m} \sum_{i=1}^m \mathbb{E} \|\nabla_v F_i(u_i^t, v_i^t)\|^2 + \frac{1}{m} \sum_{i=1}^m \mathbb{E} \left\langle \nabla_v F_i(\bar{u}^t, v_i^t) - \nabla_v F_i(u_i^t, v_i^t), v_i^{t+1} - v_i^t \right\rangle \\
&\stackrel{b)}{\leq} \underbrace{-\eta_v K_v \mathbb{E}[\Delta_v^t]}_{\mathcal{T}_{3,v}} + \underbrace{\frac{L_{vu}^2}{2m} \sum_{i=1}^m \mathbb{E} \|\bar{u}^t - u_i^t\|^2 + \frac{1}{2m} \sum_{i=1}^m \mathbb{E} \|v_i^{t+1} - v_i^t\|^2}_{\frac{1}{L_v} \mathcal{T}_{2,v}},
\end{aligned} \tag{29}$$

where a) and b) is get from the unbiased expectation property of  $\nabla_v F_i(u_i^t, v_i^t; \xi_i)$  and  $\langle x, y \rangle \leq \frac{1}{2}(\|x\|^2 + \|y\|^2)$ , respectively.

For  $\mathcal{T}_{2,v}$ , according to Lemma 2, we have

$$\begin{aligned}
\mathcal{T}_{2,v} &\leq \frac{L_v}{2} \left( \frac{16\eta_v^2 K_v^2}{m} \sum_{i=1}^m \mathbb{E} \|\nabla_v F_i(u_i^t, v_i^t)\|^2 + 8\eta_v^2 K_v^2 \sigma_v^2 \right) \\
&\leq 8L_v \eta_v^2 K_v^2 \mathbb{E}[\Delta_v^t] + 4L_v \eta_v^2 K_v^2 \sigma_v^2.
\end{aligned} \tag{30}$$

For  $\mathcal{T}_{3,v}$ , according to Eq. (25), we have

$$\frac{L_{vu}^2}{2m} \sum_{i=1}^m \mathbb{E} \|\bar{u}^t - u_i^t\|^2 \leq \frac{L_{vu}^2}{(1-\lambda)^2} \left[ 3\eta_u^2 K_u L_u^2 \rho^2 + 9\eta_u^2 K_u^2 (\sigma_u^2 + \delta^2 + 2\mathbb{E}[\Delta_u^t]) \right]. \tag{31}$$

After that, summing Eq. (29), (30), and (31), we have

$$\begin{aligned}
\mathbb{E} \left[ F(\bar{u}^t, V^{t+1}) - F(\bar{u}^t, V^t) \right] &\leq \left( -\eta_v K_v + 8\eta_v^2 K_v^2 (L_v + 1) \right) \mathbb{E}[\Delta_v^t] + 4\eta_v^2 K_v^2 \sigma_v^2 (L_v + 1) \\
&\quad + \frac{L_{vu}^2}{(1-\lambda)^2} \left[ 3\eta_u^2 K_u L_u^2 \rho^2 + 9\eta_u^2 K_u^2 (\sigma_u^2 + \delta^2 + 2\mathbb{E}[\Delta_u^t]) \right].
\end{aligned} \tag{32}$$

**Obtaining the Final Convergence Bound.**

$$\begin{aligned}
\mathbb{E} \left[ F(\bar{u}^{t+1}, V^{t+1}) - F(\bar{u}^t, V^t) \right] &= \mathbb{E} \left[ F(\bar{u}^t, V^{t+1}) - F(\bar{u}^t, V^t) + F(\bar{u}^{t+1}, V^{t+1}) - F(\bar{u}^t, V^{t+1}) \right] \\
&\leq \left( \frac{\eta_u}{2} - \eta_u K_u + \frac{54\eta_u^3 K_u^3 L_u^2}{(1-\lambda)^2} \right) \mathbb{E}[\Delta_u^t] + \frac{5}{2} \eta_u^2 K_u L_u (L_u^2 \rho^2 + \sigma_u^2 + \delta^2) \\
&\quad + \frac{3\eta_u K_u L_u^2}{2(1-\lambda)^2} (6\eta_u^2 K_u L_u^2 \rho^2 + 18\eta_u^2 K_u^2 (\sigma_u^2 + \delta^2)) \\
&\quad + \left( -\eta_v K_v + 8\eta_v^2 K_v^2 (L_v + 1) \right) \mathbb{E}[\Delta_v^t] + 4\eta_v^2 K_v^2 \sigma_v^2 (L_v + 1) \\
&\quad + \frac{L_{vu}^2}{(1-\lambda)^2} \left[ 3\eta_u^2 K_u L_u^2 \rho^2 + 9\eta_u^2 K_u^2 (\sigma_u^2 + \delta^2 + 2\mathbb{E}[\Delta_u^t]) \right].
\end{aligned} \tag{33}$$

Summing from  $t = 1$  to  $T$ , assume the local learning rates satisfy  $\eta_u = \mathcal{O}(1/L_u K_u \sqrt{T})$ ,  $\eta_v = \mathcal{O}(1/L_v K_v \sqrt{T})$ ,  $F^*$  is denoted as the minimal value of  $F$ , i.e.,  $F(\bar{u}, V) \geq F^*$  for all  $\bar{u} \in \mathbb{R}^d$ , and  $V = (v_1, \dots, v_m) \in \mathbb{R}^{d_1 + \dots + d_m}$ . We can generate

$$\begin{aligned}
\frac{1}{T} \sum_{i=1}^T \left( \frac{1}{L_u} \mathbb{E}[\Delta_u^t] + \frac{1}{L_v} \mathbb{E}[\Delta_v^t] \right) &\leq \mathcal{O} \left( \frac{F(\bar{u}^1, V^1) - F^*}{\sqrt{T}} + \frac{\sigma_v^2 (L_v + 1)}{L_v^2 \sqrt{T}} + \frac{L_u}{T} \right. \\
&\quad \left. + \frac{L_{vu}^2}{T^{1/2}(1-\lambda)^2} \left( \frac{\rho^2}{K_u} + \frac{\sigma_u^2 + \delta^2}{L_u^2} \right) + \frac{L_u}{T(1-\lambda)^2} \left( \frac{\rho^2}{K_u} + \frac{\sigma_u^2 + \delta^2}{L_u^2} \right) \right).
\end{aligned} \tag{34}$$

Assume that

$$\sigma^2 = \frac{\rho}{K_u} + \frac{\sigma_u^2 + \delta^2}{L_u^2}.$$

Then, we have the final convergence bound:

$$\frac{1}{T} \sum_{i=1}^T \left( \frac{1}{L_u} \mathbb{E}[\Delta_u^t] + \frac{1}{L_v} \mathbb{E}[\Delta_v^t] \right) \leq \mathcal{O} \left( \frac{F(\bar{u}^1, V^1) - F^*}{\sqrt{T}} + \frac{\sigma_v^2 (L_v + 1)}{L_v^2 \sqrt{T}} + \frac{L_u}{T} + \frac{\sigma^2 L_{vu}^2}{T^{1/2}(1-\lambda)^2} + \frac{\sigma^2 L_u}{K_u^2 T(1-\lambda)^2} \right). \tag{35}$$

Furthermore, When the perturbation amplitude  $\rho$  is proportional to the learning rate, e.g.,  $\rho = \mathcal{O}(1/\sqrt{T})$ , the sequence of outputs  $\Delta_u^t$  and  $\Delta_v^t$  generated by Alg. 1, we have:

$$\mathcal{O}(\sigma^2) = \mathcal{O} \left( \frac{\rho^2}{K_u} + \frac{\sigma_u^2 + \delta^2}{L_u^2} \right) = \mathcal{O} \left( \frac{1}{K_u T} + \frac{\sigma_u^2 + \delta^2}{L_u^2} \right). \tag{36}$$